ÇUKUROVA UNIVERSITY
INSTITUTE OF NATURAL AND APPLIED SCIENCES

BAHRİ BÜYÜKAKÇALI

MSc THESIS

TWO PHASE GAS-LIQUID FLOW IN HORIZONTAL TUBE WITH VARIOUS INSERTS

DEPARTMENT OF MECHANICAL ENGINEERING

ADANA, 1999

ÇUKUROVA ÜNİVERSİTESİ
FEN BİLİMLERİ ENSTİTÜSÜ

TWO PHASE GAS-LIQUID FLOW IN HORIZONTAL TUBE WITH VARIOUS INSERTS

BAHRİ BÜYÜKAKÇALI

YÜKSEK LİSANS TEZİ

MAKİNE MÜHENDİSLİĞİ ANABİLİMDALI

Bu Tez 15/09/1999 Tarihinde Aşağıdaki Jüri Üyeleri Tarafından Oybirliği ile Kabul Edilmiştir.

İmza:	İmza:	İmza:
Prof. Dr.-Ing.	Doç. Dr.	Yard. Doç Dr.
Tuncay YILMAZ	Kadir AYDIN	Osman BABAARSLAN

Bu Tez Enstitümüz Makine Mühendisliği Anabilim Dalında Hazırlanmıştır.

Kod No: 1647

Prof. Dr. Melih BORAL
Enstitü Müdürü

Bu Çalışma Çukurova Üniversitesi Araştırma Fonu tarafından Desteklenmiştir.
Proje No: FBE.99.YL.30

LIST OF CONTENTS **Page**

ABSTRACT

MSc THESIS

TWO PHASE GAS-LIQUID FLOW IN HORIZONTAL TUBE WITH VARIOUS INSERTS

BAHRİ BÜYÜKAKÇALI

DEPARTMENT OF MECHANICAL ENGINEERING
INSTITUTE OF NATURAL AND APPLIED SCIENCES
ÇUKUROVA UNIVERSITY

Supervisor : Prof. Dr. –Ing. Tuncay YILMAZ

Jury : Prof. Dr. –Ing. Tuncay YILMAZ
Doç. Dr. Kadir AYDIN
Yard. Doç. Dr. Osman BABAARSLAN

Two-phase flow in pipes is often encountered in engineering applications. A liquid containing gas bubbles flowing in a pipe of different cross-sectional area is a simple example of two-phase gas-liquid flow.

In this study, gas-liquid flows in horizontal pipes for inserted and non-inserted pipes are examined to fill up this deficiency in literature. In the first step, experimental results will be compared with empirical methods. Especially slug flows will be examined in a detailed manner using both empirical calculation methods and experimental results. Therefore, differences between flow parameters of inserted and empty pipe will be investigated. Particularly, variations of flow regimes with respect to gas, liquid flow rates and eccentricity of two pipes will be determined.

Key words: Two phase flow, flow in horizontal pipe, gas liquid flow

ÖZ

YÜKSEK LİSANS TEZİ

İÇİNDE ÇEŞİTLİ EK CİSİMLER BULUNAN YATAY BORULARDA İKİ FAZLI GAZ SIVI AKIŞININ İNCELENMESİ

BAHRİ BÜYÜKAKÇALI

ÇUKUROVA ÜNİVERSİTESİ
FEN BİLİMLERİ ENSTİTÜSÜ
MAKİNE MÜHENDİSLİĞİ ANABİLİMDALI

Danışman : Prof. Dr. -Ing. Tuncay YILMAZ

Jüri : Prof. Dr. –Ing. Tuncay YILMAZ
Doç. Dr. Kadir AYDIN
Yard. Doç. Dr. Osman BABAARSLAN

Mühendislik uygulamalarında sıkça meydana gelen iki fazlı akışa en basit örnek, bir boru içerisinde gaz ve sıvının beraberce akmasıdır.

Bu çalışmada yatay boş boruda ve borunun içine yerleştirilen eklerle elde edilen akış geometrileri incelenecektir. İlk olarak, boş boruda yapılan deney sonuçları literatürdeki bir takım metotlarla karşılaştırılacaktır. Bu çalışmada özellikle slug tipi akış incelenecektir. Bu tip akışta elde edilen deneysel sonuçlar boş boru ve ekli boru için karşılaştırılacak ayrıca bu akış tipine boru içine yerleştirilen eklerin etkisi araştırılacaktır.

Anahtar kelimeler: İki fazlı akış, yatay boruda akış, gaz sıvı akışı

THANKS

I wish to express my thanks to my supervisor Prof. Dr.-Ing. Tuncay YILMAZ for his supports and encouragement throughout this study.

Special thanks to Assoc. Prof. Dr. Orhan BÜYÜKALACA for his guidance.

I should also thanks to my work mates; Res. Ass. Hasan DANIŞMAN, Res. Ass. Akif TOPCUOĞLU, Res. Ass. Gülhan KAPLAN, Res. Ass. İbrahim TAPAN, Res. Ass. Alper BULCA.

In addition, I wish to express my special thanks to my family for their endless support during my whole life.

LIST OF FIGURES **Pages**

LIST OF TABLES **Pages**

LIST OF SYMBOLS

Symbols

u_G	Superficial gas velocity	(m/s)
u_L	Superficial liquid velocity	(m/s)
A	Cross-sectional area of the empty tube	(m^2)
ρ_g	Gas density	(kg/m^3)
ρ_l	Liquid density	(kg/m^3)
$\dot{M}_g$	Gas mass flow rate	(kg/s)
$\dot{M}_l$	Liquid mass flow rate	(kg/s)
u_g	Actual gas velocity	(m/s)
u_l	Actual liquid velocity	(m/s)
A_g	Void fraction	-
V	Volume of the tube	(m^3)
V_g	Gas volume	(m^3)
V_l	Liquid volume	(m^3)
$\Delta P_{l,1}$	Single phase pressure loss of liquid	(Pascal)
$\Delta P_{g,1}$	Single phase pressure loss of gas	(Pascal)
M_w	Water mass flow rate	(kg/s)
M_g	Gas mass flow rate	(kg/s)
K	Overall pressure loss	(Pascal)
β	Ratio of throat diameter to inlet diameter	-
C_d	Ratio of real flow rate to theoretical flow rate	-
$\overline{U}$	Average velocity of the fluid	(m/s)
Q_{real}	Actual flow rate	(kg/s)
ΔP	Pressure drop	(mmWG)
Q_{th}	Theoretical flow rate	(kg/s)

1. INTRODUCTION

Two-phase flow in pipes is often encountered in engineering applications. Typical industrial applications where two-phase gas-liquid flow occurs are boilers, condensers, heat exchangers, air-conditioning and refrigeration equipments, distillation columns, desalination, nuclear reactors, rocket motors, chemical reactors, high temperature metallurgical processes including steel making, transportation of petroleum and other plants in power and process industries. A liquid containing gas bubbles flowing in a pipe of different cross-sectional area is a simple example of two-phase gas-liquid flow. Various flow regimes are seen in multiphase flow. These include stratified, wavy, plug, slug, bubbly and annular flow regimes(Yılmaz, 1998).

The accurate prediction of multiphase flow characteristics is required in the flow lines for their safe design and economical operation. Gas-liquid flows in conduits may take on a variety of configurations related to the spatial distribution of the two phases in the pipe termed as flow patterns. In gas-liquid flow systems where the interface between the phases can have very complex forms, there seems to be no immediate prospect of achieving a completely satisfactory theoretical model. One of the most complex flow pattern with unsteady characteristics is the intermittent or slug flow. Gas-liquid intermittent flow exists in the whole range of pipe inclinations and over a wide range of gas and liquid flow rates. In vertical slug flow most of the gas is located in large bullet-shaped bubbles which occupy most of the pipe cross section. These bubbles are called Taylor bubbles. The Taylor bubbles are separated by liquid slugs usually containing small bubbles. The liquid confined between the bubble and the pipe wall flows around the Taylor bubble in a thin falling film. In horizontal and inclined flow, slugs of liquid that fill the whole cross section of the pipe are separated by a stratified zone with an elongated gas bubble in the upper part of the pipe and the liquid film at the bottom (Kakaç and Mayinger, 1976).

Slug flow is a highly complex type of flow with an unsteady nature, thus the prediction of pressure drop, heat and mass transfer for such flow is a difficult task. A variety of approximate methods has been developed for calculating hydrodynamic parameters of the slug. The older methods simply used correlations of experimental results. More recently there is a tendency to formulate approximate models that is capable of simulating the flow behavior sufficiently accurate so that the calculation of the pressure drop as well as other flow parameters can be performed with a relatively high degree of confidence and generality.

The prediction rates in oil and gas wells are such that in most cases, the multiphase flow lines are normally in slug flow. An important example of gas-liquid two-phase flows is slug flow, in which large bubble plugs separate liquid slugs. Due to momentum of the slugs, mechanical forces and vibrations can occur in the pipe system. Approaching eigen frequency of the pipe system, the slug frequency can couse resonance. So, slug flow develops to increase pipe damage from internal corrosion and mechanical impacts e.g. in a pipeline, pumps are subjected to very strong fluctuations that can have destructive effects.

Gas-liquid flows in horizontal and vertical pipes have been examined by many researchers. However, there are only limited number for studies of flow in concentric pipes. Two- phase flow in eccentric vertical pipes has been investigated only by Kelessidis and Dukler (1987). However, no study has been found in the literature related to two phase flows in horizontal eccentric pipes.

In this study, gas-liquid flows especially slug flow in horizontal pipes with inserts and without inserts are examined to fill up the deficiency in the literature. The structure and pressure drop of slug flows are examined in a detailed manner using various measurement devices. Differences between pipe flow parameters for with insert and without insert are investigated. Particularly, variation of flow regimes with respect to gas, liquid flow rates and eccentricity of inserts are determined. The main set of experiments include all four types of flow rate changes, i.e. increasing gas, decreasing gas, increasing liquid and decreasing liquid flow rate.

2. LITERATURE REVIEW

The requirement of economic designs, optimization of operating conditions, and assessment of safety factors lead to the need for quantitative information for two-phase flow takes place in a wide range of industrial plant. Competition in capital and operating costs, and the importance of reliability and safety have accentuated this need. However, two-phase flow is not a subject that can be treated successfully by purely theoretical methods. Therefore, many researchers have tackled to get reliable experimental data to determine the flow patterns, pressure drop, velocity distribution and void fraction in tubes. Two-phase gas liquid flows can occur in pipes that are vertical, horizontal or inclined configurations. The investigations in the literature are summarized given below for such kinds of configurations.

Experimental methods in multiphase flows have been explained and some representative examples of measurements in two-phase turbulent flows have been given by Bachalo (1994). Prediction, measurement and detection of flow patterns, void fractions, bubble velocities and bubble sizes for two-phase flows in vertical and horizontal tubes have been investigated entirely and several methods and measurement devices have been proposed, designed and tested by many researchers (Iida 1980, McQuilan 1980, Kocamustafaoğulları 1994, Sheng 1991, Din 1987.

Intermittent, or slug flow, is a very common occurrence in gas-liquid two-phase pipe flow and in many applications slug flow is an undesirable flow pattern since the existence of long lumps of liquid slugs move at high speed which is unfavorable to gas-liquid transportation (Barnea, Taitel 1993). Considerable efforts have been devoted to the prediction of the slug hydrodynamic characteristics. Finally, Barnea, Taitel have suggested a model for the slug length distribution at various positions along the pipe. Experimental investigation of upward gas-liquid slug flow in a vertical pipe has been carried out and the results of measuring of the local void fraction, liquid velocity and components of liquid velocity fluctuations have been presented by Nakoryakov (1986). As a conclusion of Nakoryakow's study, the time-dependent behavior of the instantaneous hydrodynamic characteristics are described. A design of conductivity probe for the measurement of void fraction has been developed and tested for slug flow regime in vertical air-water flows and flow patterns ranging from bubbly to annular flows were observed by Costiga (1997) and Barnea (1989). A new predictive model for slug/churn transition has been presented and the predicted boundary has been compared with experimental results. This predictive model shows satisfactory agreement with experimental results of Brauner (1986).

A gas-liquid two-phase upward flow system with a flow obstacle has been investigated to elucidate the effects of obstacle on film thickness (Kavakami 1980 and Fukano 1980). These works present an experimental and analytical approach to understand the film thinning mechanism during the drainage.

An experimental study of droplet size and velocity distributions in gas-liquid annular upflow has been reported for vertical tubes including the effects of liquid viscosity and the radial variation of drop size and velocity (Fore 1995). In this investigation, the authors have concluded that the mean drop sizes observed increase with increasing of liquid flow rate and viscosity.

The liquid phase turbulent structure of an air-water, bubbly upflow in a circular pipe has been investigated experimentally by Liu and Bankoff (1993). The experimental set-up of these studies has been designed to make possible the simultaneous measurement of the local velocities, void fraction, bubble velocity, bubble size distribution and turbulent stresses using both one and two dimensional hot-film anemometer probes. In these works, the important experimental results and parametric trends are summarized and discussed and the data are compared with some other data sources and existing models.

Experiments on the propagation of small void fraction disturbances along an upward vertical test section have been reported by Jabardo and Boure (1989) for bubbly flows and transitional (bubbly-slug) flows. In particular, it is shown that two propagation phenomena, with different speeds, may coexist, the higher speed wave being closely correlated with the appearance of slugs.

Experimental studies of air-water two-phase flow in helically coiled vertical tubes have been carried out to clarify the liquid-film thickness, pressure drop and void fraction (Whalley 1980, Saxena 1990,Watanabe 1993).

Experiments have been performed by Sadatomi and Sato (1982) for vertical two-phase flow of air-water mixtures through several noncircular channels. In particular, flow pattern boundaries have been presented and the data obtained.

Two-phase flow in concentric and eccentric annuli occurs in a variety of important practical situations. For example; the influx of the gas into the wellbore of an oil well creates two-phase flow in an annulus and during the measurements in oil wells, the presence of the instrument creates annular passages. Better understanding of this phenomena will provide more reliable design methods for many types of industrial equipment. From this view point, the importance of subject has been considered and the investigations to model the flow pattern transitions for upward vertical two-phase flow in concentric and eccentric tubes have been published by Sekoguchi (1981), Kelessidis and Dukler (1989),

Many of experimental studies for two-phase gas-liquid flow in horizontal tubes are related to determination of flow patterns, phase distributions and measurement of void fraction, film thickness and pressure drop (Choi 1995, Fan 1993, Barnea 1993, Hand 1993.

Gas-liquid mixtures flowing in horizontal rectangular channels have been studied to determine the range of occurrence of flow patterns and pressure drop by Troniewski(1984) and Wambsganss (1991).

Helicoidal pipes are used extensively in engineering applications and experimental investigations have been conducted for air-water two-phase flow in horizontal helicoidal pipes of varying configurations by Awwad (1995).

Commercial pipelines consist mainly of uphill and downhill inclined sections. This actual situation has been directed the researchers to examine the effect of pipe inclination on flow patterns, liquid hold up and pressure drop for gas-liquid two-phase flow in inclined tubes (Stanislow 1986, Andreussi 1989).

No study has been found in the literature related to two-phase flows in horizontal eccentric pipes.

In this study, gas-liquid flows in horizontal pipes for eccentric and centric pipes and for plate inserts are examined to fill up this deficiency in the literature. In the first step, experimental results will be compared with empirical methods.

Especially slug flows will be examined in a detailed manner using both measurement devices. Therefore, differences between eccentric and centric pipe flow parameters will be investigated. Particularly, variations of flow regimes with respect to gas, liquid flow rates and eccentricity of two pipes will be determined.

3. MATERIAL AND METHOD

3.1. FLOW PATTERN

The analysis of single-phase flow is made easier if it can be established that the flow is either laminar or turbulent. This information is equally important and useful in the study of multi- phase flow especially gas-liquid flow. Much more important is the flow pattern that is the topology of the flow for gas-liquid flows. The particular flow pattern depends on the condition of pressure, flow, heat flux and channel geometry. In the design of a heat exchanger it is desirable to know what the flow pattern or successive flow pattern is so that a hydrodynamic or heat transfer theory appropriate to that pattern can be chosen (Yılmaz, 1998).

The gas and liquid phases may assume different geometrical configurations when flowing simultaneously. One phase may be dispersed while the other is continuous, or both phases may be stratified. Such flow configurations are usually termed two-phase flow pattern or flow regimes. A change of flow pattern means a change in the mode of transport of momentum or heat.

One of the most important points about two-phase flow is that, in a transparent channel one can apparently see what is going on. When the flow is rapid, it is an easy matter to take high speed films and this extends the range of visual observation and interpretation.

There is considerable disparity in the description of visual observations given by different authors. Some of the names that have been given to regimes in liquid-gas co-current flow based on visual observations are bubbly, gas dispersed, gas piston, liquid slug, annular, liquid dispersed, froth slugging, mixed frothy, wall film, mist, aerated, piston, churn, wave entrainment, drop entrainment, semi annular, stratified, wavy, and they are many more. Here we classify the flow patterns in terms of the most commonly accepted terms and descriptions. It is necessary to define the flow regimes independently for vertical and horizontal flow.

3.1.1 Flow Pattern in Vertical Flow

3.1.1.1. Flow Pattern

The main flow patterns in vertical upward flow are illustrated in figure 3.1. In bubbly flow the gas phase is distributed in discrete bubbles within the liquid phase. This regime is the easiest to imagine from everyday experience. At one extreme, the bubbles may be small and spherical and at the other extreme the bubbles may be large with a spherical cap and a flat tail.

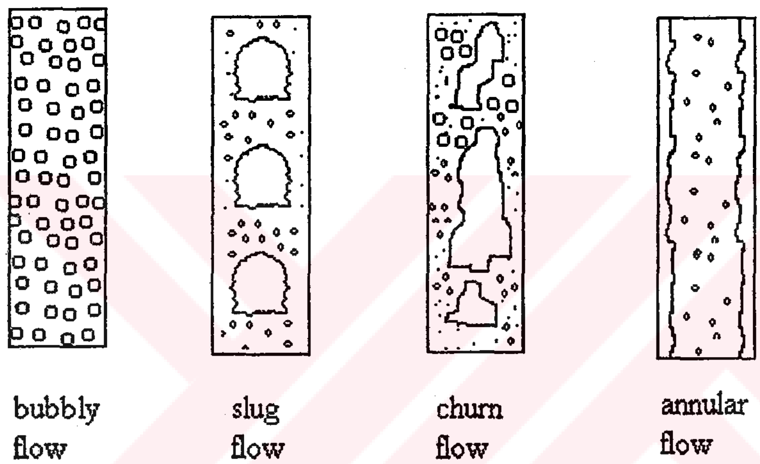

Figure 3.1. Flow patterns in vertical flow

In slug flow the gas or vapor bubbles have nearly the same cross-section as that of the duct and move along in the characteristic bullet-shaped bubbles. The nose of the bubble has a characteristic spherical cap and the gas in the bubble is separated from the pipe wall by a slowly descending film of liquid. The liquid flow is contained in liquid slugs which separate successive gas bubbles. The bubbles of gas are separated by lengths occupied mainly by liquid which may or may not contain dispersion of smaller gas bubbles.

Churn flow is formed by the breakdown of the large vapor bubbles in slug flow. The gas or vapor flows in a more or less chaotic manner through the liquid which is mainly displaced to the channel wall. The flow has an oscillatory or time varying character. Hence, the descriptive name is churn flow. This flow pattern is also sometimes named as semi-annular or slug-annular flow. The transition region between the slug flow and annular flow is sufficiently well marked and specific to be given a separate identity and the name churn flow is given to it.

In annular flow a liquid film forms at the tube wall with a continuous central gas or vapor core. Large amplitude waves are usually present on the surface of the film and the continuous break up of these waves forms a source for droplet entrainment which occurs in varying amounts in the central gas core. The liquid film may or may not contain gas bubbles and the core may or may not contain liquid droplets.

3.1.1.2. Flow Pattern Map

Despite the present deficiencies in the understanding of the various flow patterns and the transitions from one pattern to another, there is a need for simple methods to give some idea of the particular pattern likely to occur for a given set of local flow parameters. One method of representing the various transitions is in the form of a flow pattern map. The respective pattern may be presented as areas on a graph, where the coordinates are superficial velocities $\mathbf{u_G}$ and $\mathbf{u_L}$ which are defined as follows:

$$\mathbf{u_G} = \frac{\dot{M}_g}{\rho_g . A} \quad ; \quad \mathbf{u_L} = \frac{\dot{M}_l}{\rho_l . A} \qquad (3.1)$$

Here are A the cross-sectional area of the empty tube, ρ_g and ρ_l the gas and liquid density $\dot{M}_g$ and $\dot{M}_l$ gas and liquid mass flow rate respectively.

Instead of $\mathbf{u_G}$ and $\mathbf{u_L}$ one can have generalized or dimensionless parameters containing these superficial velocities. The flow pattern is also influenced by a number of secondary variables but it is impossible to represent their influence using only a two dimensional plot.

Sometimes one uses instead of the superficial velocities $\mathbf{u_G}$ and $\mathbf{u_L}$ the actual velocities $\mathbf{u_g}$ and $\mathbf{u_l}$. The definition of them are:

$$u_l = \frac{\dot{M}_l}{\rho_l A_l} = u_L \frac{A}{A_l} = \frac{u_L}{1-\alpha}$$
$$u_g = \frac{\dot{M}_g}{\rho_g A} = u_G \frac{A}{A_g} = \frac{u_G}{\alpha} \qquad (3.2)$$

The area averaged gas fraction $\mathbf{A_g}$ is referred to as the void fraction;

$$\alpha = \frac{V_g}{V} = \frac{A_g}{A} \quad ; \quad 1-\alpha = \frac{V_l}{V} = \frac{A_l}{A} \qquad (3.3)$$

Here, V is the volume of the tube, V_g and V_l are gas and liquid volumes in this tube.

The total mass flow M is given for one component two-phase flow. For this case, one can define a mass quality ;

$$\dot{x} = \frac{\dot{M}_g}{\dot{M}} \quad ; \quad 1-\dot{x} = \frac{\dot{M}_l}{\dot{M}} \qquad (3.4)$$

using this mass quality, the velocities can be calculated from equation 3.1 as follows:

$$u_G = \frac{\dot{M}.\dot{x}}{\rho_g . A} \quad ; \quad u_L = \frac{\dot{M}.(1-\dot{x})}{\rho_l . A} \qquad (3.5)$$

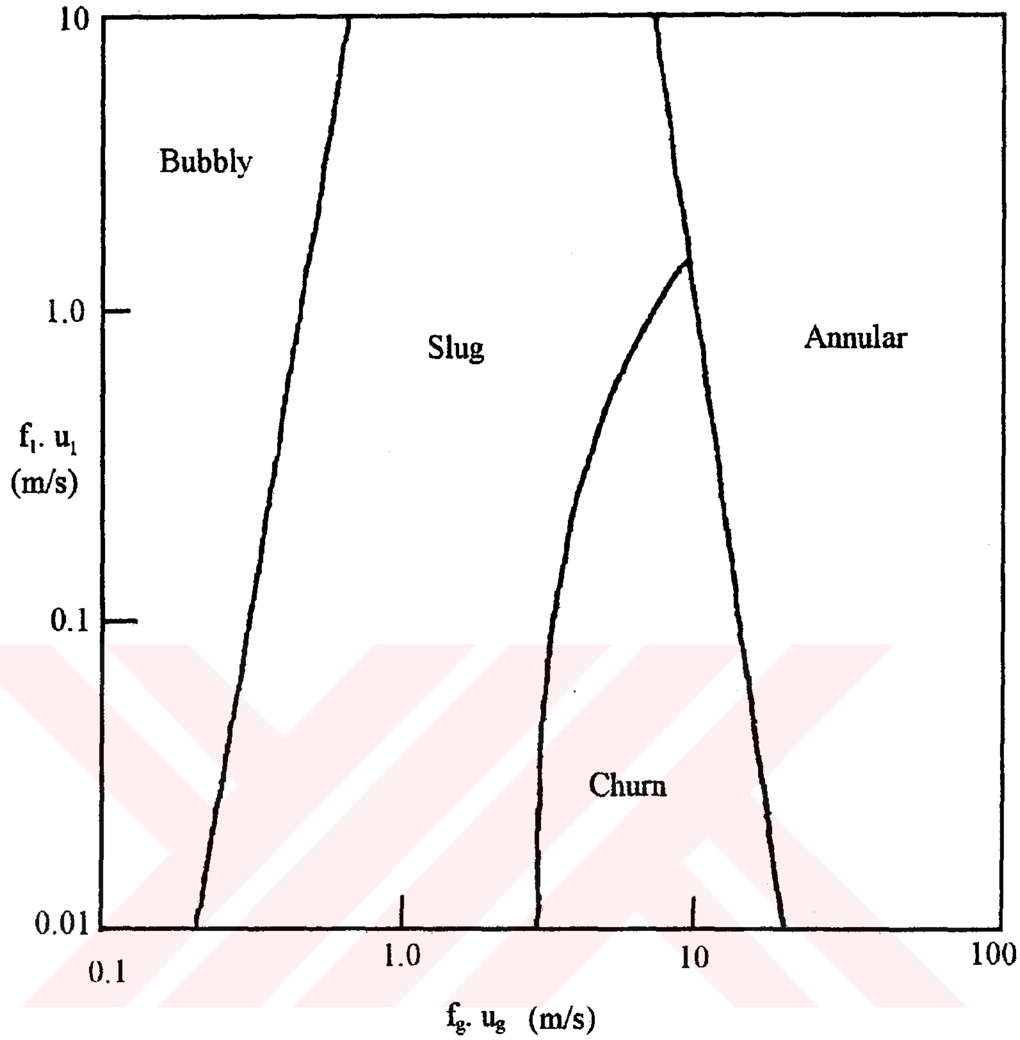

Figure 3.2 Flow patterns map for vertical flow

In figure 3.2 the flow pattern map for vertical upflow is given based on the work of Govier and Aziz (1972). In this graph f_l and f_g are defined as follows:

$$f_l = \left(\frac{\rho_l}{\rho_{l_1}} \frac{\sigma_1}{\sigma}\right)^{1/4} \quad ; \quad f_g = \left(\frac{\rho_g}{\rho_{g_1}}\right)^{1/3} . f_l \qquad 3.6)$$

in which ρ_g and ρ_l are densities of the gas and liquid phase respectively and σ is the surface tension. The subscript 1 in these equations indicates the values of the physical properties at a temperature of 15.5 °C. According to this diagram, at low mass flow rates of gas flow, bubbly flow condition will be obtained. As mass flow rate of gas increases, flow types becomes slug, churn and annular respectively.

3.1.2 Flow Pattern in Horizontal Flow

3.1.2.1 Flow Pattern

The flow pattern in co-current two-phase flow in horizontal and inclined tubular channels are complicated by asymmetry of the phases resulting from the influence of the gravity. The generally accepted flow patterns are shown schematically in figure 3.3.

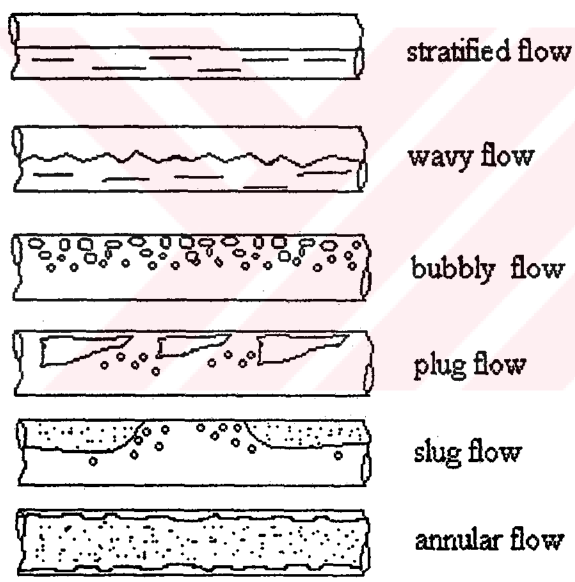

Figure 3.3. Flow patterns in horizontal flow.

Stratified flow pattern only occurs at very low liquid and vapor velocities. The separation of the liquid and gas phases is complete, the liquid flowing at the bottom of the tube and the gas at the top. The two phases have a relatively smooth interface.

In wavy flow pattern one can see large surface waves. These waves develop from the stratified flow pattern when the gas velocity is increased.

Bubbly flow in horizontal flow is similar to that in vertical flow except that the vapor bubbles tend to travel in the upper half of the pipe. At moderate velocities of both vapor and liquid phases, the entire pipe cross-section contains bubbles whilst at still higher velocities a flow pattern equivalent to the wispy-annular pattern is entered. This pattern is sometimes referred to as froth flow.

Plug flow is similar to slug flow in the vertical case but the liquid layer separating the gas bubbles from the wall tends to be thicker at the bottom of the pipe than at the top.

Slug flow condition can be seen by further increasing of the gas velocity in the wavy flow regime. Increased gas velocity causes the waves at the interface to be picked up to form a frothy slug which is propagated along the pipe at a high velocity. The upper surface of the tube behind the wave is wetted by a residual film which drains into the bulk of the liquid.

Annular flow originates from the slug flow when the gas velocity is increased. In this case a gas core forms with a liquid film around the periphery of the pipe. The film may or may not be continuous around the entire circumference but it will of course, be thicker at the base of the pipe.

Flow in inclined channels is of technological importance in some designs of boiler and in oil pipelines. The flow pattern in such tubes tend to lie between those for vertical and horizontal flow, the asymmetry increasing as the horizontal position is approached.

Flow patterns formed during the generation of vapor in horizontal tubular channels are influenced by departures from thermodynamic and hydrodynamic equilibrium. Figure 3.4 shows a schematic representation of a horizontal tubular channel heated by a uniform low heat flux and fed with liquid just below the saturation temperature. Important points to note from a heat transfer viewpoint are the possibility of intermittent drying and rewetting of the upper surfaces of the tube in slug and wavy flow and the progressive drying out over long tube lengths of the upper circumference of the tube wall in annular flow. At higher inlet liquid velocities the influence of gravity is less obvious, the phase distribution becomes more symmetrical and the flow patterns become closer to those seen in vertical flow.

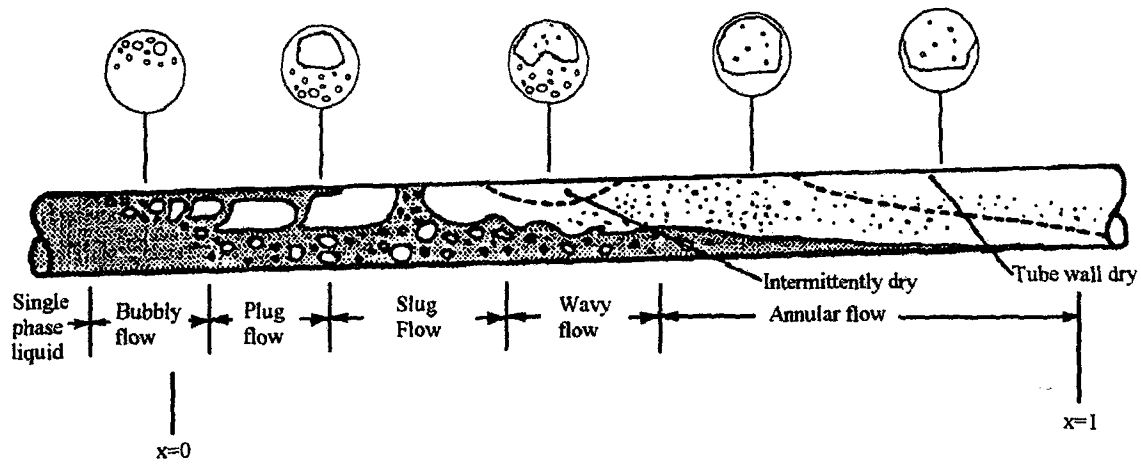

Figure 3.4. Flow patterns in a horizontal tube evaporator

3.1.2.2 Flow Pattern Map

For horizontal tube, the best-known and most used flow regime map is that of Baker (1954). This map is shown in figure 3.5.

The parameters in the figure, λ and ψ on the axes are defined as follows:

$$\lambda = \left(\frac{\rho_A}{\rho_g}\frac{\rho_W}{\rho_l}\right)^{1/2} \qquad (3.7)$$

$$\psi = \left(\frac{\sigma_W}{\sigma}\right)\left(\frac{\mu_l^2}{\mu_W^2}\frac{\rho_W}{\rho_l}\right)^{1/3}$$

The subscripts **A** and **W** refer to the values of the physical properties for air and water respectively at atmospheric pressure and temperature. Although the Baker chart serves as a useful qualitative guide to flow pattern in horizontal flow, the actual results can deviate very significantly from it.

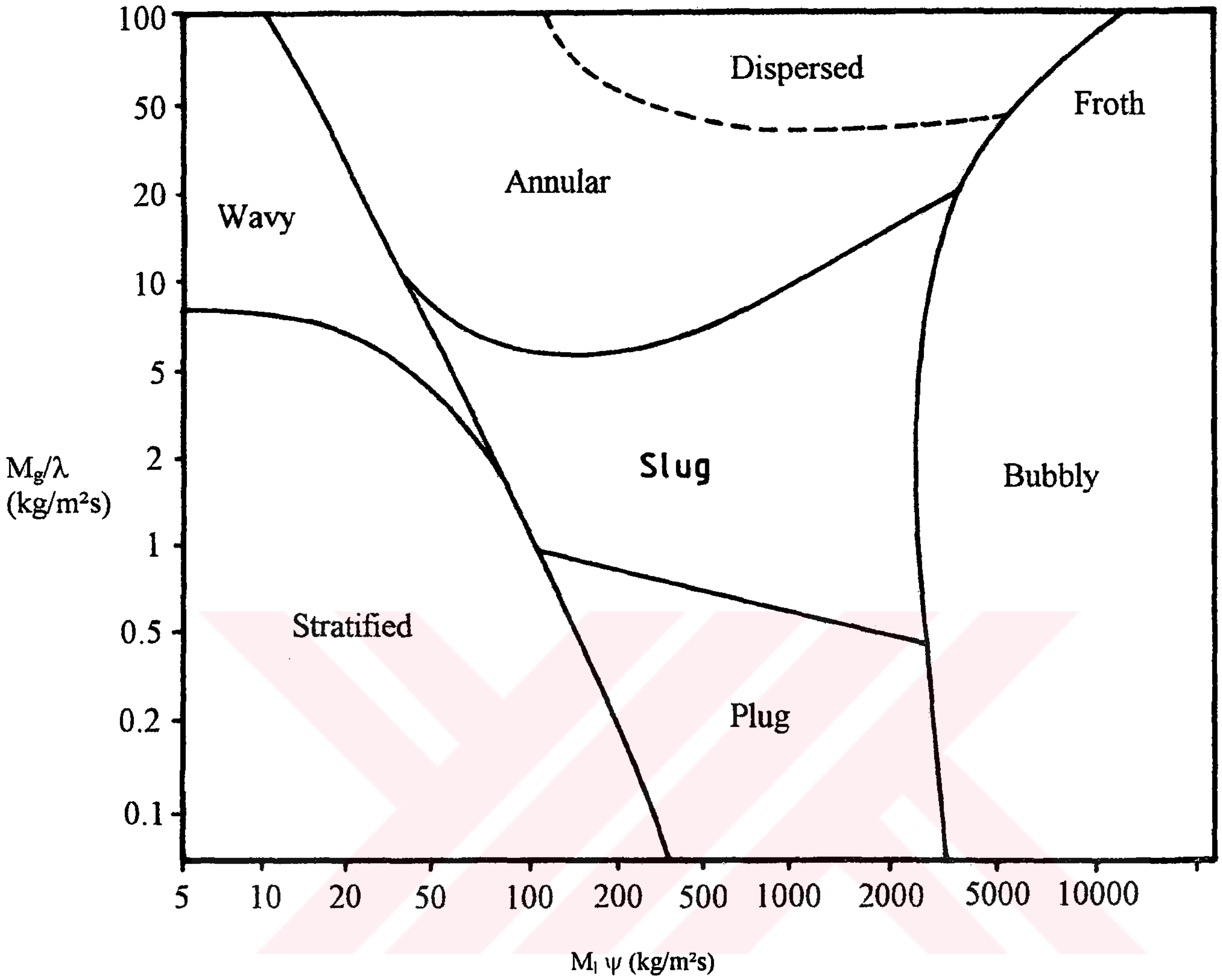

Figure 3.5. Flow pattern map for horizontal flow

3.2. EMPIRICAL METHODS of TWO PHASE FLOW

Here, generalized correlations are discussed for the frictional pressure drop and void fraction in gas-liquid flow. Generalized correlations are used here in the sense of not being flow pattern oriented, or restricted to a particular flow pattern.

3.2.1. The Lockhart-Martinelli Method (LMM)

Lockhart-Martinelli method is one of the well known methods to calculate pressure drop and void fraction. The method was developed for horizontal two-phase flow of two component system at low pressure. In this method, a definite portion of the flow area is assigned to each phase and it is assumed that conventional friction pressure drop equation can be applied to the flow path of each phase (Lockhart and Martinelli, 1949).

In this method two-phase friction multipliers ϕ_l and ϕ_g are defined as follows:

$$\phi_l = \sqrt{\frac{\Delta P}{\Delta P_{l,1}}} \quad (3.8)$$

$$\phi_g = \sqrt{\frac{\Delta P}{\Delta P_{g,1}}} \quad (3.9)$$

The multipliers ϕ_l and ϕ_g are the square roots of the ratio of two-phase pressure loss to the single phase pressure loss of liquid ($\Delta P_{l,1}$) and gas ($\Delta P_{g,1}$) phase respectively.

The multipliers are expressed dependent on the parameter **X** defined as;

$$X = \sqrt{\frac{\Delta P_{l,l}}{\Delta P_{g,l}}} \quad (3.10)$$

ϕ_l and ϕ_g are given dependent on **X** for four different conditions. These can be described using the following formulas;

$$\phi_l^2 = 1 + \frac{C}{X} + \frac{1}{X^2} \quad (3.11)$$

$$\phi_g^2 = 1 + CX + X^2 \tag{3.12}$$

C has the following values for different flow conditions in table 3.1.

Table 3.1. Flow conditions and constant C

Liquid	Gas	Notation	C
Turbulent	Turbulent	(TT)	20
Laminar	Turbulent	(LT)	12
Turbulent	Laminar	(TL)	10
Laminar	Laminar	(LL)	5

The void fraction can be described by;

$$\alpha = 1 - \frac{1}{\phi_{l,tt}} \tag{3.13}$$

Where $\phi_{l,tt}$ is to be calculated from equation (3.11) with **C=20**. Another equation for α is; (Yılmaz, 1998).

$$\alpha = \frac{1}{(1 + X^{0.8})^{0.378}} \tag{3.14}$$

According to these formulations, pressure losses calculated for different mass flow rates of water and air are shown in figure 3.6 for the test section designed in this study.

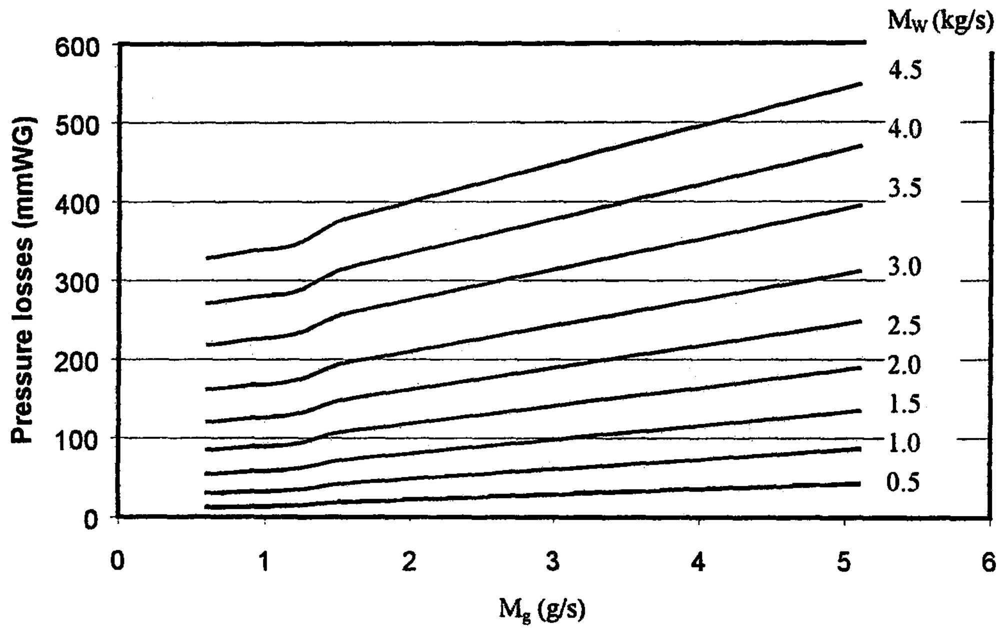

Figure 3.6. Variation of pressure loss with air flow rate according to LMM, for the test section designed in this study.

3.2.2. The Chisholm Method (CM)

In this method, the equation for **LMM** is used. Only constant **C** is to be calculated from the following equation (Chisholm, 1983):

$$C = (2^{2-n} - 1)\Gamma - \frac{1}{\Gamma} \qquad (3.15)$$

Here, **n** is referred to the superscript in the Blasius-type friction equation. For Blasius equation **n=0.25** and this equation reduces to

$$C = 2.364\Gamma - \frac{1}{\Gamma} \qquad (3.16)$$

where Γ is defined as follows:

$$\Gamma = \sqrt{\frac{\Delta P_{tg,1}}{\Delta P_{tl,1}}} \qquad (3.17)$$

$\Delta P_{TL,1}$ and $\Delta P_{TG,1}$ are the pressure losses in single-phase flow, if one assume that all gas and liquid flows as a liquid or as a gas. If we have turbulent-turbulent flow **C=20** and therefore **LMM** should be used only if Γ >**8.5**. Below this value of Γ, equation 3.16 is recommended.

The variation of pressure loss with mass flow rate of air for different values of water flow rate is shown in figure 3.7 according to CM for the test section designed in this study.

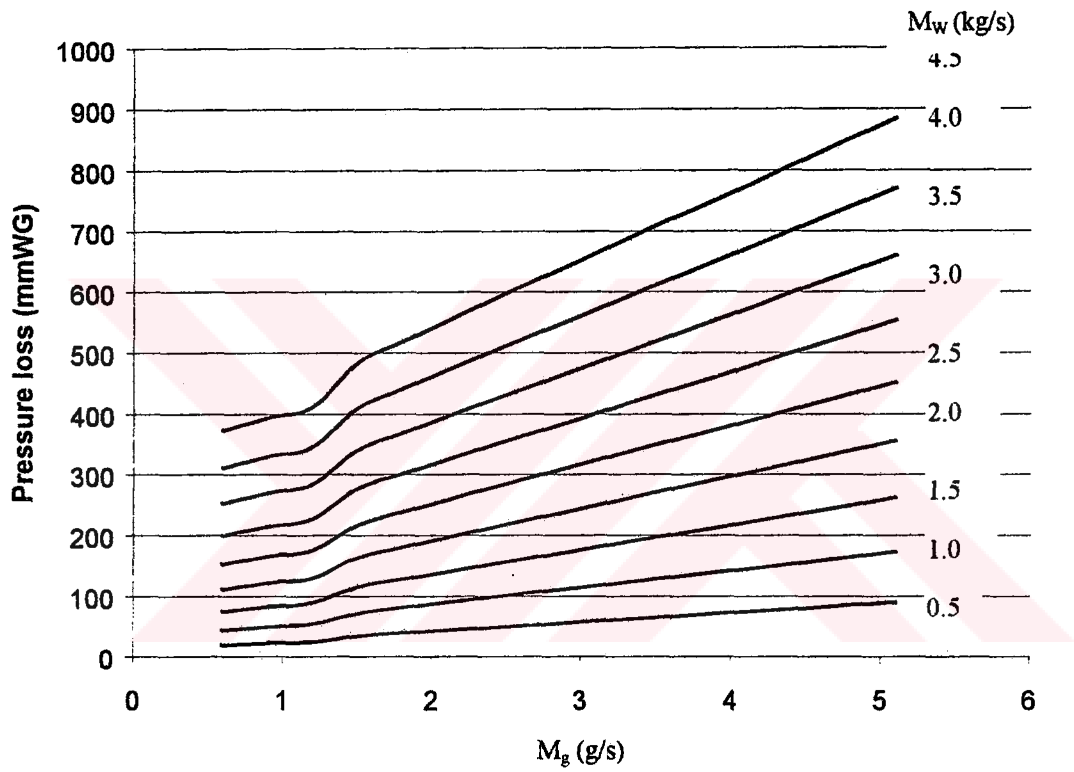

Figure 3.7. Variation of pressure loss with air mass flow rate according to CM, for the test section designed in this study.

3.2.3. The Boroczy-Chisholm Method (BCM)

In this method (Chisholm, 1973) a two-phase multiplier $\phi_{TL,1}$ is defined;

$$\phi_{TL,1}^{2} = \frac{\Delta P}{\Delta P_{TL,1}} \tag{3.18}$$

This multiplier is to be determined from the following equation:

$$\phi_{TL,1} = 1 + (\Gamma^2 - 1)\cdot\left[B\cdot \dot{x}^{0.9}\cdot(1-\dot{x})^{0.9} + \dot{x}^{1.8}\right] \quad (3.19)$$

For the parameter B the following values should be used:

Table 3.2. Variation of parameter B

Γ	$\dot{m}$ (kg/m^{2}s)	B
<0.95	<500	4.8
	500-1900	2400/m
	>1900	$55/\dot{m}^{0.5}$
0.95-28	≤ 600	$520/\left(\Gamma \dot{m}^{0.5}\right)$
	>600	21/Γ
>28	-	$15000/\left(\Gamma^2 \dot{m}^{0.5}\right)$

The variation of pressure loss with mass flow rate of air is shown in figure 3.8 according to BCM for the test section designed in this study.

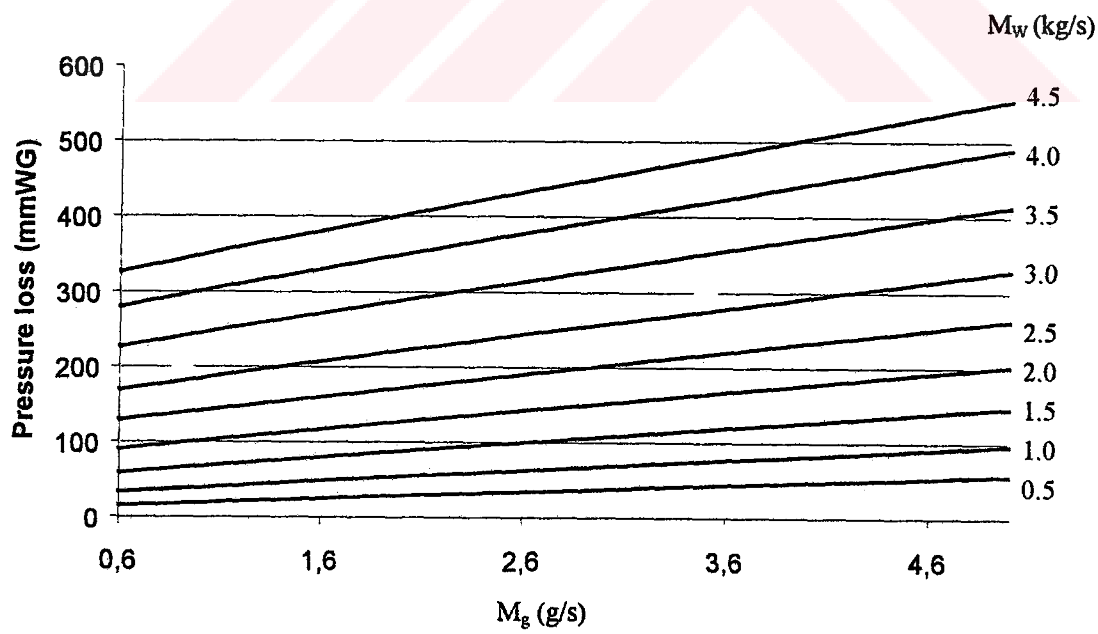

Figure 3.8. Variation of pressure loss with air mass flow rate according to BCM, for the test section designed in this study.

3.3. EXPERIMENTAL SETUP AND PROCEDURE

The experiments are performed using the experimental setup shown in figure 3.9. In the experimental setup, the water in the storage tank flows down to the test section through a 6 m height water feed line. Then, it is mixed with air. Air and water flow rates are measured separately before mixing. The air-water mixture passes through the test section which is a transparent plexiglass tube. Flow visualization and measurement of pressure loss of two phase flow are performed at the test section. Air and water are separated in a separation tank. The remaining water flows to a dump tank, while air passes to atmosphere. The water from the dump tank is pumped using a centrifugal pump to the storage tank on the roof. The rate of the flow is adjusted manually by a valve.

The air supply to the setup is provided by the main air system of the laboratory through a calibrated venturimeter. Air flow rate is controlled by a valve which is at the upstream of the venturimeter. The air is injected into the test section using a special injector. The separation tank is also used for calibration of the water flow rate measuring system which also based on a venturimeter. Flow rate of the water is controlled by a control valve positioned upstream of the venturimeter.

The test section is a plexiglass tube having an inside diameter of 40 mm, a wall thickness of 5 mm, and an overall length of 6 m. Upstream of the test section, there is a hydrodinamically development section of 2 m. The inside diameter of the development section is 53mm. Pressure tabs are installed along the test section 41.5 cm apart to measure pressure drop in multiphase flow. Pressure drop and flow rates of air and water are measured by a pressure transmitter and data stored in a PC.

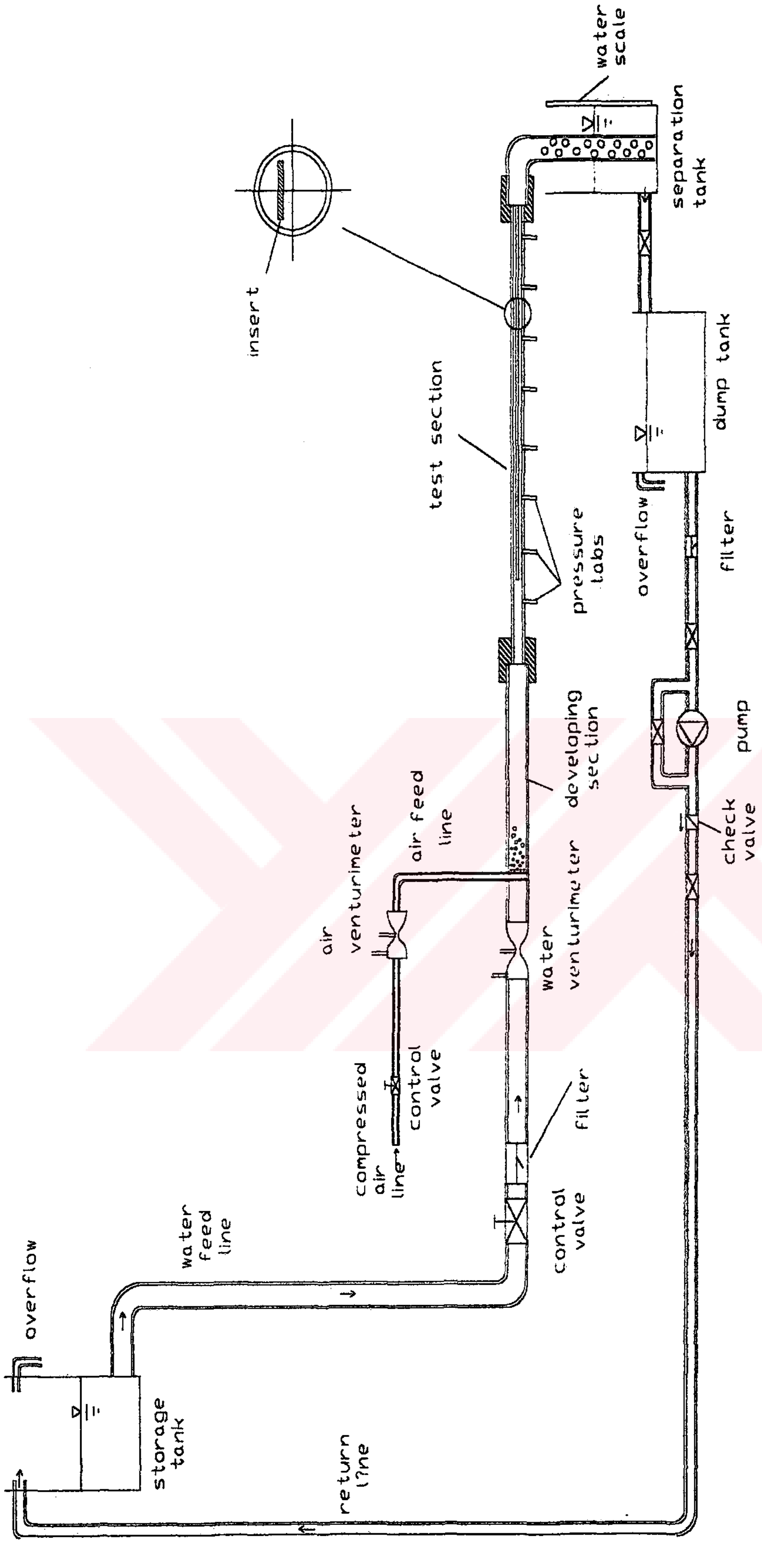

Figure 3.9. Schematic view of the experimental setup

3.3.1. AIR-WATER TWO PHASE FLOW SECTION

Two phase flow section is illustrated in figure 3.10. A 53 mm ID and 1.8 m length galvanized pipe is set upstream of the test section for the development of two-phase flow. The test section are consisted of 40 mm ID and 6 m length plexiglass transparent pipe and its connections. The plexiglass pipe and the galvanized pipe are connected to each other with a metal-PVC joint element. The transparent pipe allows us to observe the flow to be able to decide which pattern we have along the test section. The test section is made of 3 pieces of 2 m length plexiglass pipe and the pipes are fitted by specially made joints. A total of 15 pressure tabs are installed along the test section to measure the pressure drop. The distance between the tabs is 41.5 cm.

The water passed through the test section drains into the separation tank through a specially designed draining pipe which enables smooth draining without disturbing the water level inside the separation tank. The separation tank is also used for calibrating water flow rate measurement system. The volume of the tank is 0.1 m^3 and a water level measurement scale exist on it.

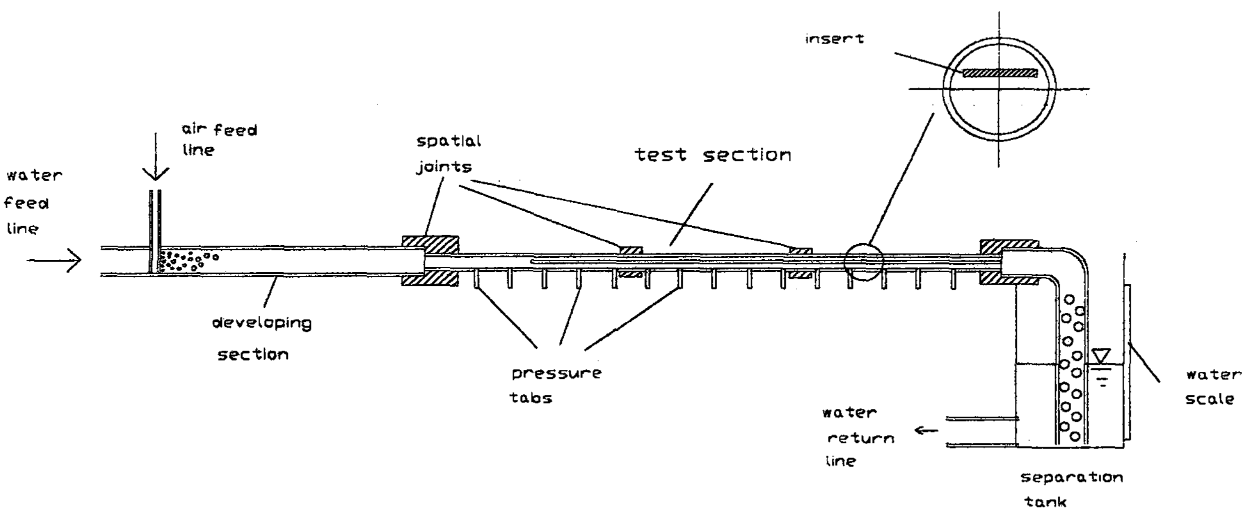

Figure 3.10. Air-water two phase flow section

The joints on the system are designed so that it's possible to replace various inserts into the test section. The inserts tested in this study are shown in figure 3.11.

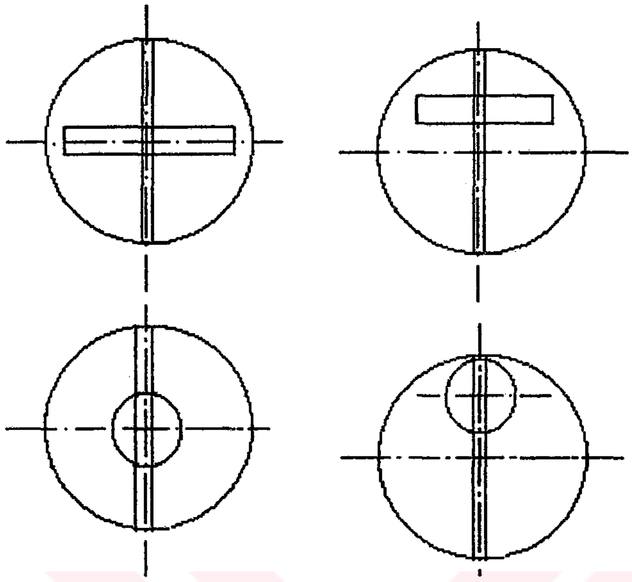

Figure 3.11. The inserts tested in this study

3.3.2. SINGLE PHASE LIQUID FLOW SECTION

Single phase liquid flow section is shown in figure 3.12. Water is supplied to the test section from 0.3 m^3 storage tank which is made of galvanized plate. The tank is replaced 6 m above the test section and connected to the test section with 53 mm ID galvanized pipe. Flow rate of the water is adjusted by a control valve and it is measured by a venturimeter. At the downstream of the control valve, a filter is used to prevent the fouling inside the test section.

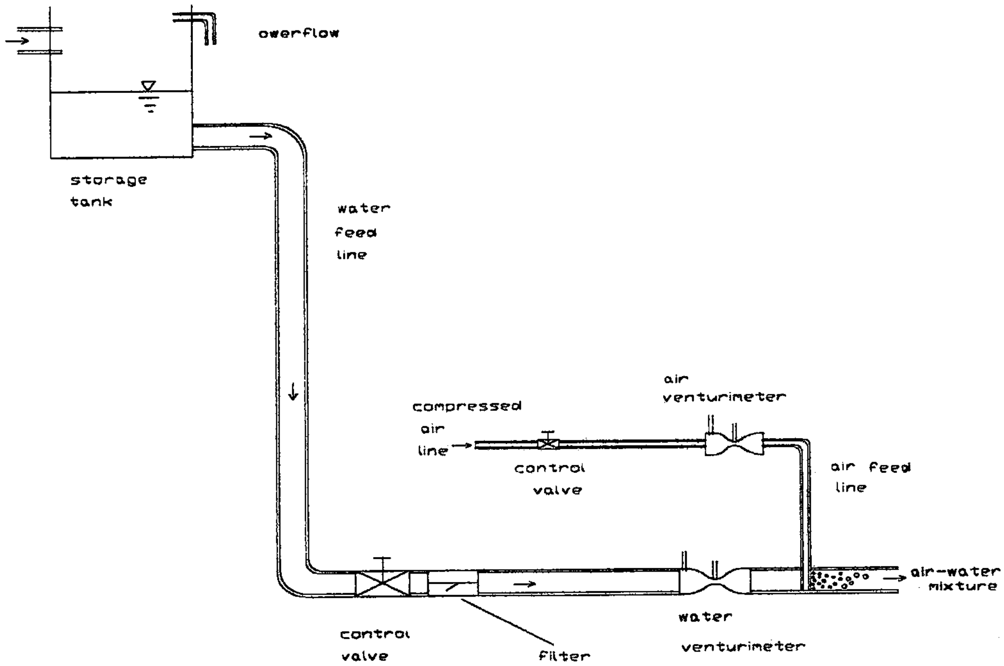

Figure 3.12. Single phase air and water flow sections

3.3.3. SINGLE PHASE AIR FLOW SECTION

Single phase air flow section is shown in figure 3.12. Air which is supplied to the test section from main compressed air system of the laboratory is controlled by a control valve. Its flow rate is measured by the means of a venturimeter. Details of the venturimeters are given in section 3.3. At the end of the air line, a specially manufactured air distribution pipe is used to inject the air into water and shown in figure 3.13. 2 mm diameter holes with 2mm distance from each other are drilled on the one side of 16 mm diameter pipe parallel to the water flow direction.

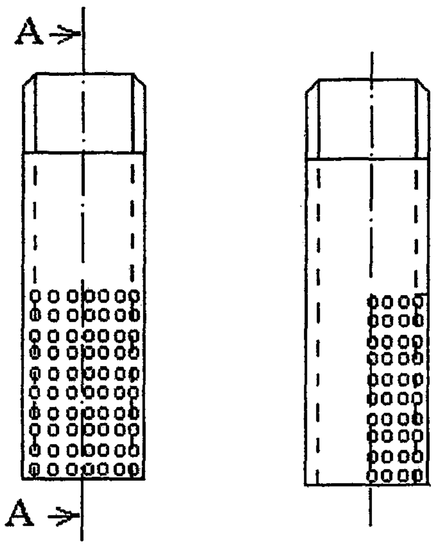

Figure 3.13. Air injection pipe

3.3.4. RETURN SECTION

The schematic view of the return section is shown in figure 3.14. The water air mixture passing through the test section into the separation tank has a volume of 0.1 m^3 . The water then flows into the dump tank with a volume of 0.25 m^3 . Filter is replaced downstream of the dump tank. The water from the dump tank is pumped back to the storage tank through the return line. Two parallel connected pump are used to pump the water from the dump tank to the storage tank on the roof of the laboratory. Pumps are capable of creating 20mWG head and 15m^3/h volume flow rate. In general, one pump is enough for experiments. However for high flow rates two of them are used.

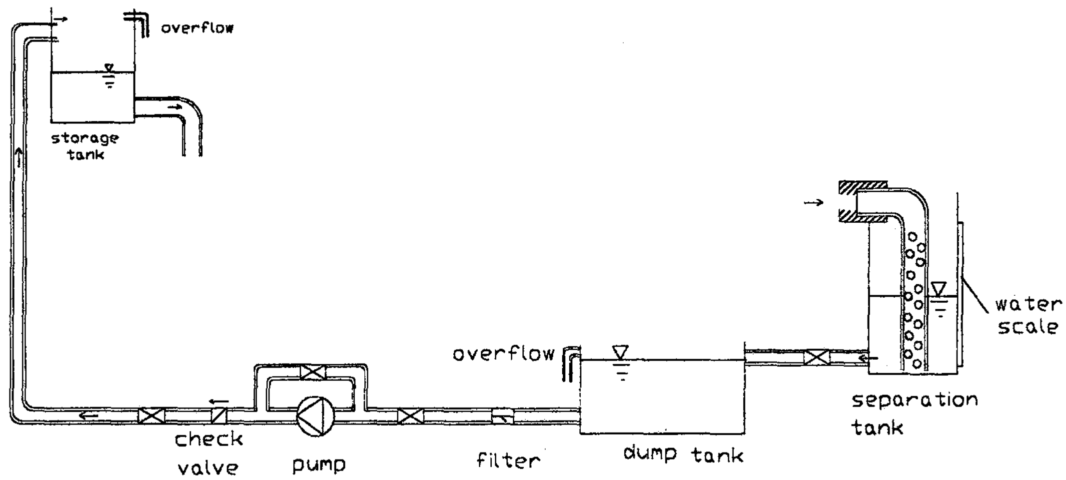

Figure 3.14. Schematic view of the return section

3.3.5. MEASUREMENT SYSTEM

General view of the measurement system is shown in figure 3.15. The test section is designed to measure pressure losses from 15 points along the test section. Flow rates of air and water also measured from venturimeter. Due to the measuring the pressure loss, 15 taps are drilled at the bottom of the plexiglass pipes which has 41.5 cm distance between each other. From these taps, plastic pipes are used to transmit pressures to the pressure transmitter. Pressure loss is measured from the points of 13th and 15th. Two pressure transmitters are used to measure pressure loss at test tube, air venturimeter and water venturimeter. The signals are stored in a PC by means of a data logger.

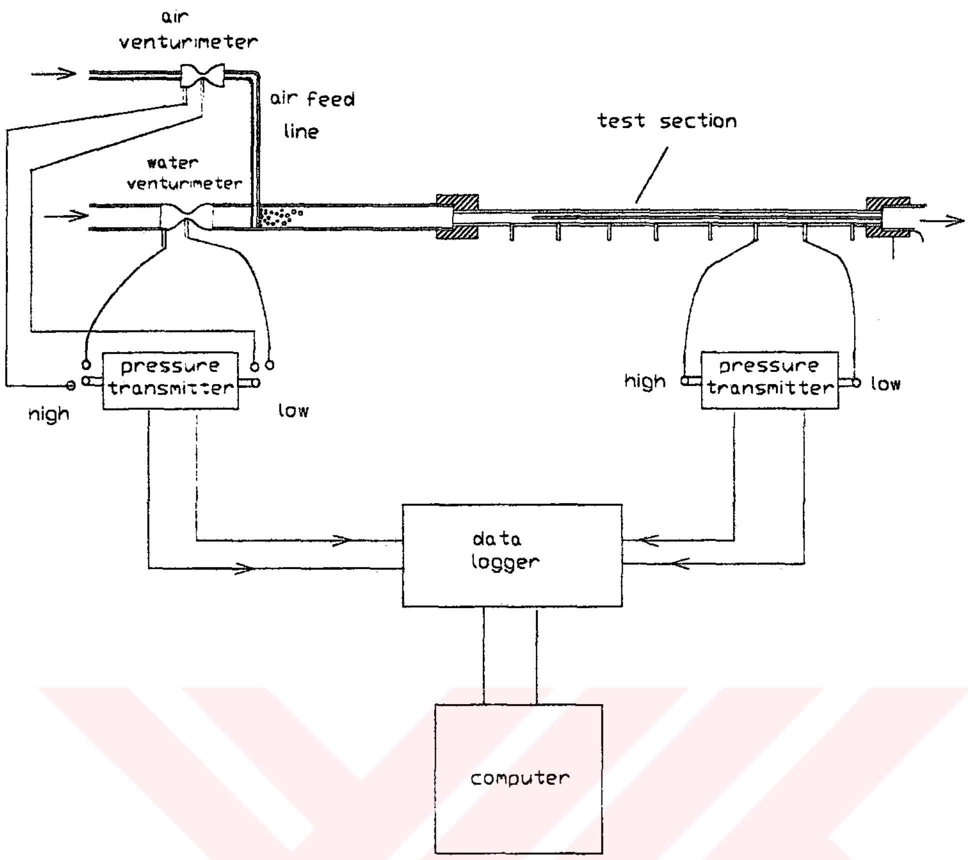

Figure 3.15. General view of the measurement system

3.3.5.1. Pressure Measurement

Pressure through the test section and through the venturimeter used for the determination of air and water flow rate are measured using pressure transmitters. The properties of the transmitter are given below.

Pressure range : 0-700 mmWG.

Accuracy : ± 1 % full scale

Output :4-20 mA or 1-5 VDC

Temperature range (compensated) : 0 to 50 °C

Power : 24 VDC

Media compatibility : clean, inert, non corrosive gases or liquids.

The electric connection of the pressure transmitter is shown in figure 3.16.

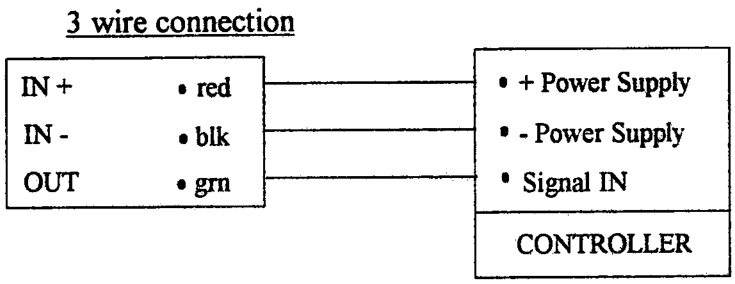

Figure 3.16. Electrical connection of pressure transmitter

The connection of the pressure transmitter to the data collection system is shown in figure 3.17.

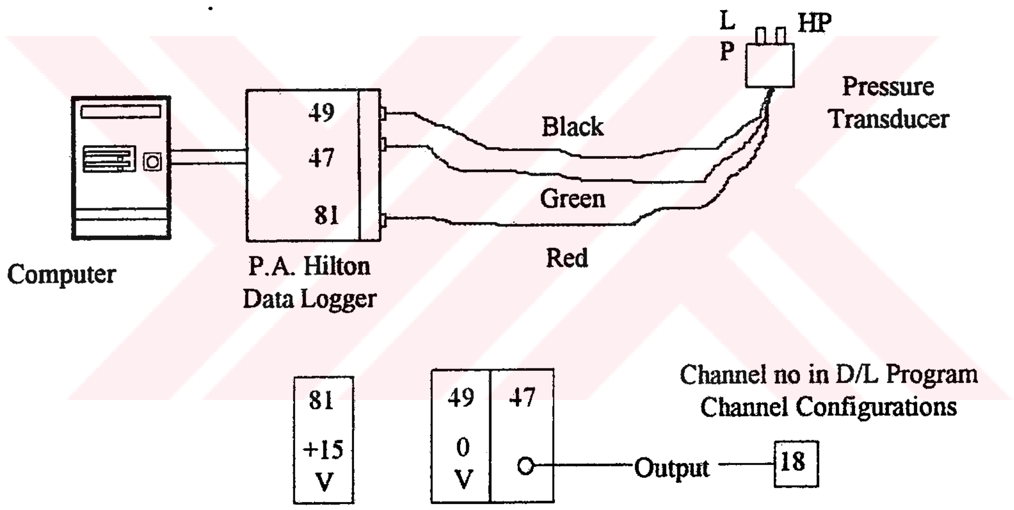

Figure 3.17. Electrical connection of the pressure transmitter to the data collection unit

The pressure transmitters are calibrated using a standard manometer. For this purpose, the pressure drop of single phase water flow through the test section is measured. After the calibration studies, a linear calibration curve which is shown in figure 3.18.

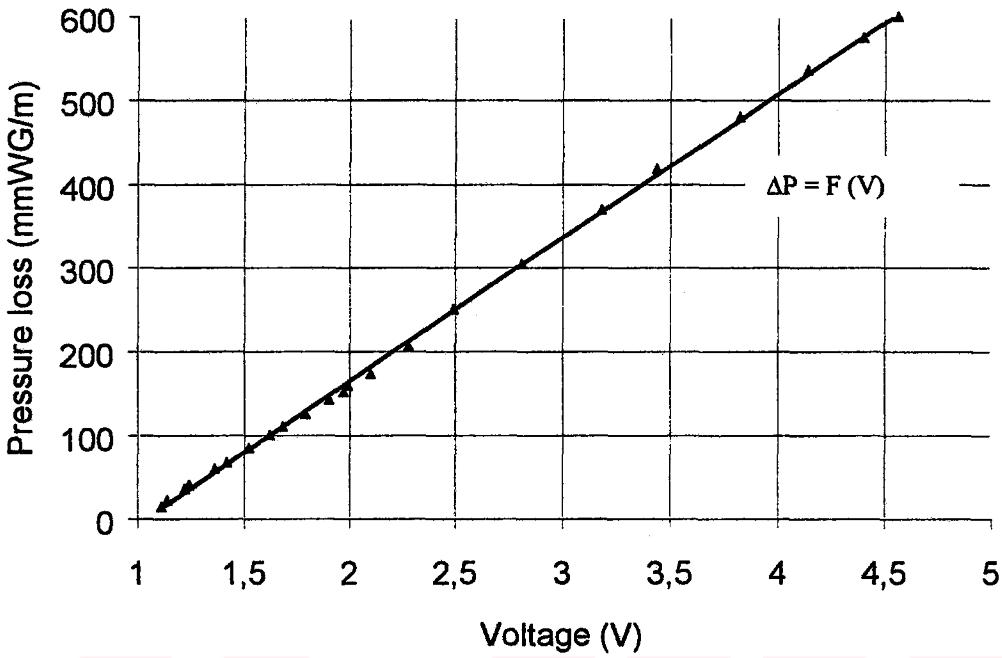

Figure 3.18. Calibration curve of the pressure transmitter.

3.3.5.2. Flow rate measurement

Different devices are available to measure flow rates of fluids. These devices split into two classes, mechanical instruments and head loss instruments (White, 1994). One of the head loss instruments is venturimeter. If pressure losses are undesirable, venturimeters are usable for flow rate measurement. The overall pressure loss of a venturimeter is shown in figure 3.19. Here **K** is overall pressure loss and β is the ratio of throat diameter to inlet diameter. In this figure, the curve of A is drown for 21° cone angle and B is drown for 8° cone angle.

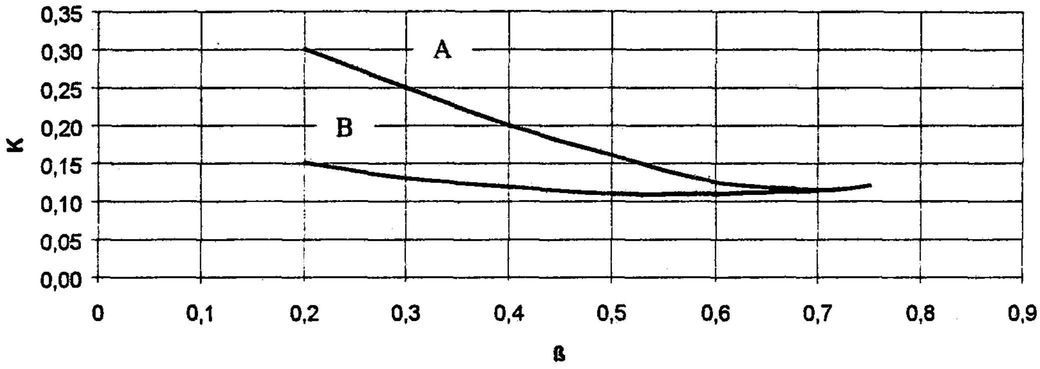

Figure 3.19. Overall pressure loss through venturimeter.

A simple shape of venturimeter is shown in figure 3.20. The inlet section consists of a short cylindrical section joined by an easy curvature to a truncated cone having an included angle of 21°. The inlet cone is joined by another smooth curve to a short cylindrical section called throat. The exit from this throat section leads by another easy curve into the exit or diffuser cone, the recommended included angle of it is 7 to 8 °. The recommended dimensions of a venturimeter are given below.

The ratio of throat section diameter (d) to entrance diameter (D) must be grater than ß=0.224 D and smaller than ß=0.742D.

The throat section length must be equal to throat diameter and pressure tap must be middle of the throat section. The throat section should be made from corrosion resistant material.

The convergent entrance length should be Lu=2.7(D-d) because the truncated cone angle is 21°.

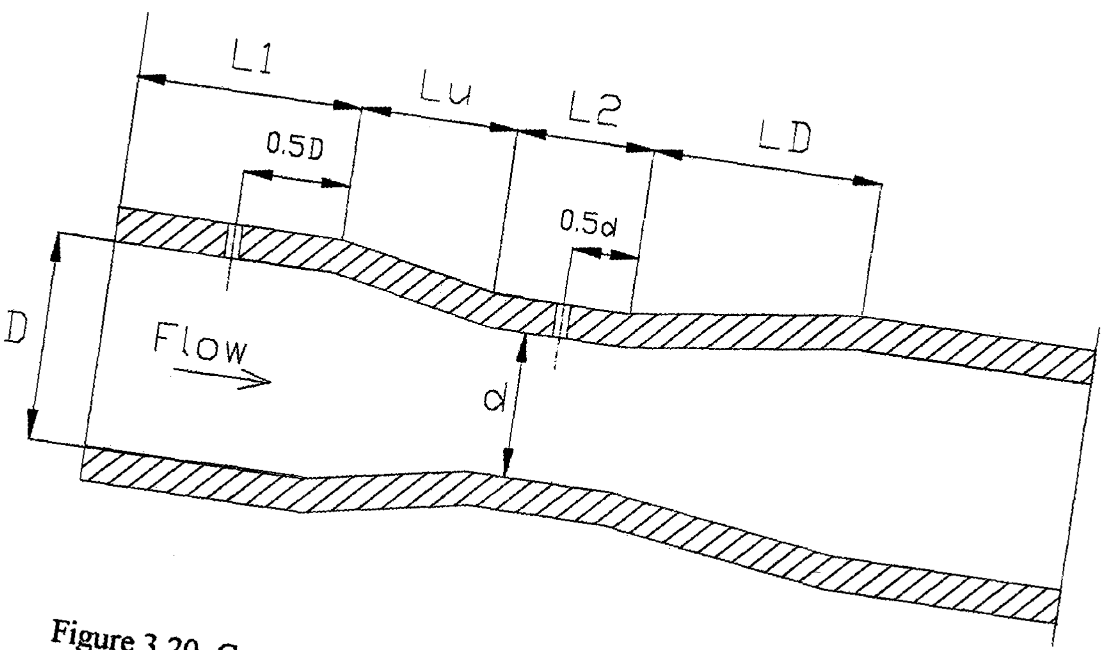

Figure 3.20. General view of a venturimeter

The divergent outlet length of venturimeter must be greater than LD=1.5 d. Because of the angle of diffuser cone should be 7 to 8 °.

The most important criteria of flow rate measurement with venturimeter is discharge coefficient (C_d). Theoretically this coefficient is nearly $0.9858-0.196\beta^{4.5}$ (White, 1994). C_d is the ratio of real flow rate to theoretical flow rate:

$$C_d = \textbf{Real flow rate / Theoretical flow rate} = \frac{Q_{real}}{Q_{th}} \qquad 3.20$$

From here, the real volume flow rate;

$$Q_{real} = C_d \cdot Q_{th}$$

From Bernoulli equation Q_{th} is;

3.21

$$Q_{th} = \frac{(\pi d^2)/4}{\sqrt{1-\beta^4}}\sqrt{\frac{2\Delta P}{\rho}}$$

3.22

$$Q_{real} = \frac{\pi D^2}{4}\overline{U} = \frac{\pi D^2}{4}\frac{U_{max}}{2}$$

Here $\overline{U}$ is average velocity of the fluid. 3.23

Substituting equation 3.22 and 3.23 substitute into equation 3.21;

$$C_d = \frac{1}{2\sqrt{2}}\left(\frac{1}{\beta}\right)^2\left(1-\beta^4\right)^{0.5}\frac{1}{\sqrt{\Delta P^*}} \qquad 3.24$$

Here, ΔP^*;

$$\Delta P^* = \frac{\Delta P}{\rho U^2_{max}} \qquad 3.25$$

3.3.5.3. Water venturimeter used for the measurement of water flow rate.

The dimensions of the water venturimeter is shown in figure 3.21. The C_d coefficient of the water venturimeter is obtained. For this purpose, the actual flow rate (Q_{real}) is obtained from the separation tank. The theoretical flow rate (Q_{th}) is calculated using the equation 3.22. The pressure drop (ΔP) through the venturimeter which is required for the calculation of Q_{th} is measured using a manometer. After all, C_d coefficient can be found using equation 3.21.

Figure 3.22 shows the variation of pressure drop through the venturimeter with the real water flow rate.

The calculated C_d values for various Re numbers and shown in figure 3.23. However, we did not obtain a curve for the C_d, since we used a pressure transmitter for the measurement of the pressure drop through the venturimeter and we calibrated the output of transmitter according to the real water flow rate. The C_d is included in this calibration. The results are shown in figure 3.24.

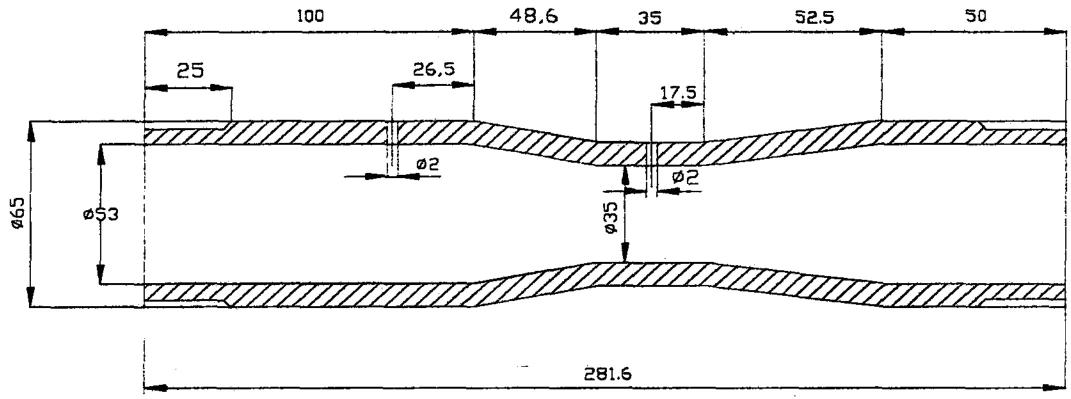

Figure 3.21. Water venturimeter and dimensions

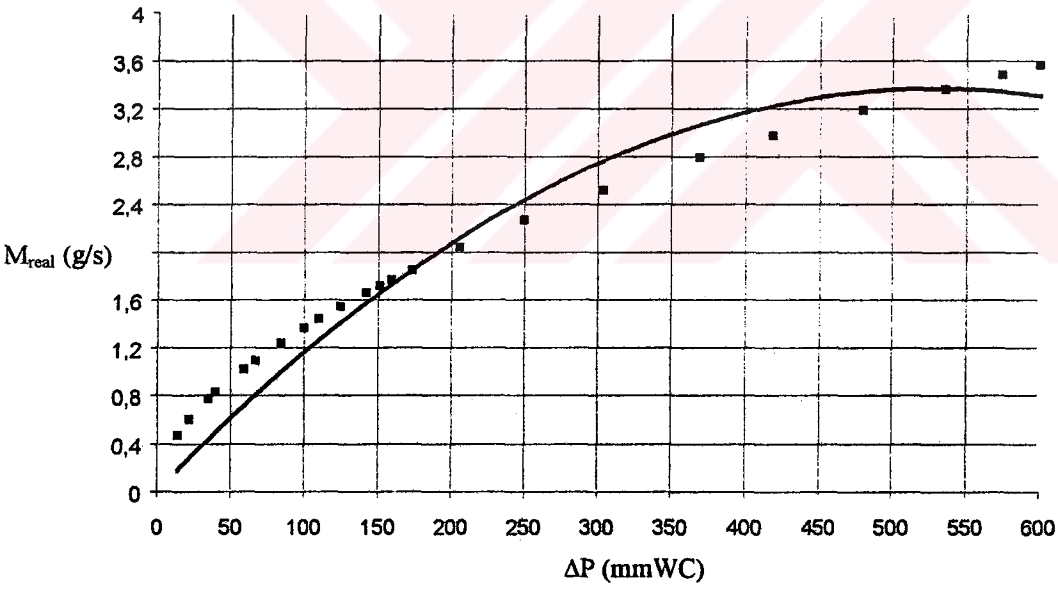

Figure 3.22. Pressure losses and mass flow rate of water in venturimeter.

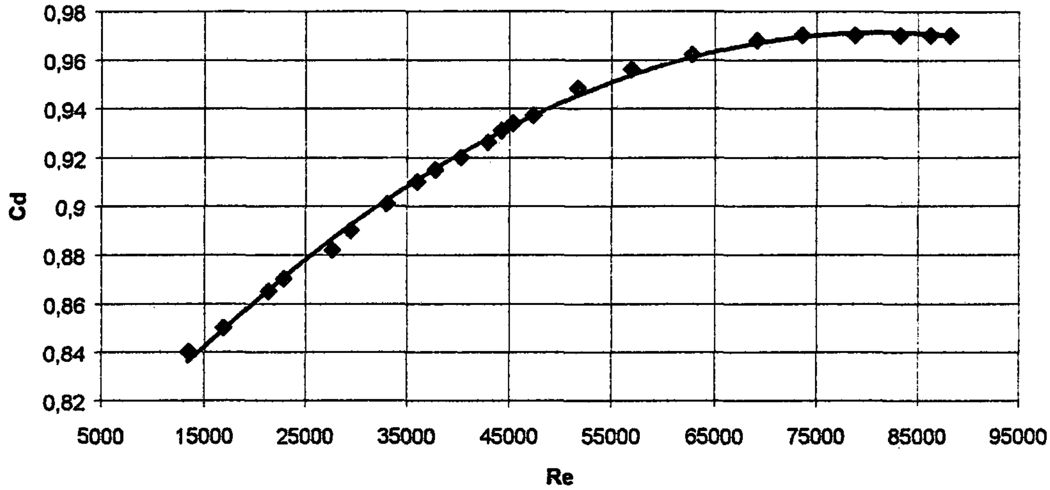

Figure 3.23. Variation with Re of discharge coefficient

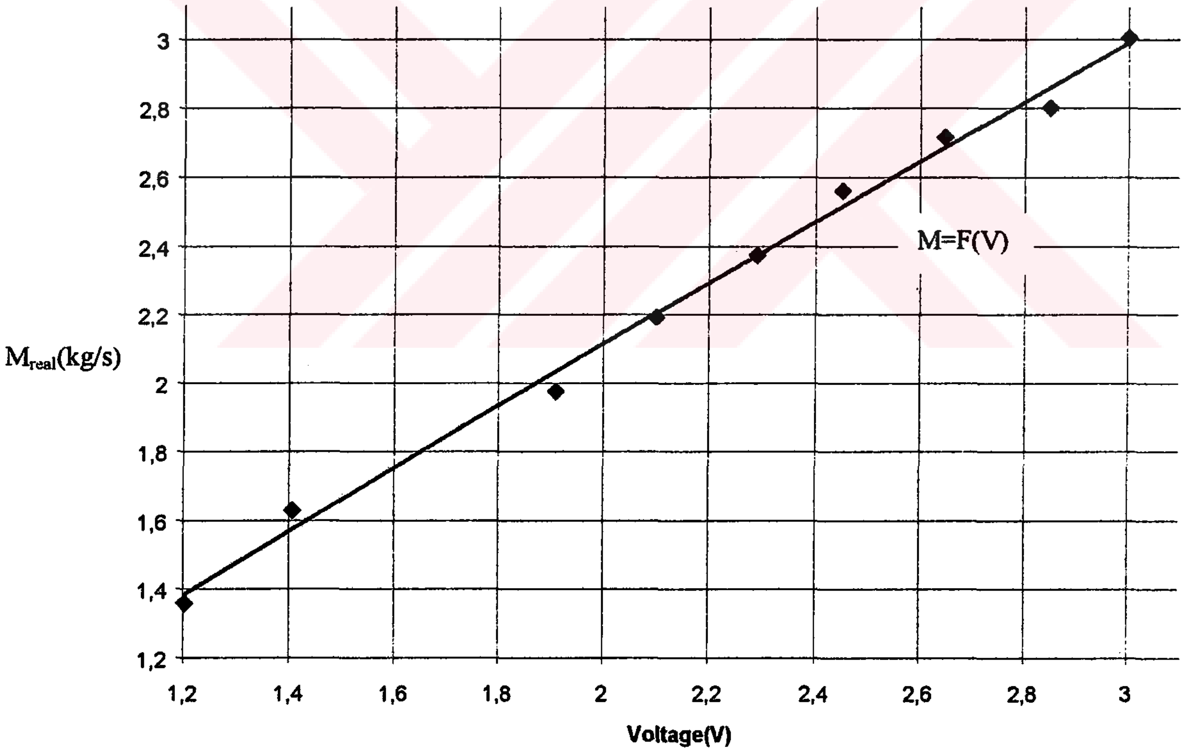

Figure 3.24. Voltage output of the pressure transmitter for various values of water flow rate.

3.3.5.4. Air Venturimeter used for the measurement of air flow rate

The dimensions of the air venturimeter is shown in figure 3.25. The air venturimeter is calibrated by using of water. The C_d coefficient of the water venturimeter is obtained. For this purpose, same procedures are followed with water venturimer. The actual flow rate (Q_{real}) is obtained from the separation tank. The theoretical flow rate (Q_{th}) is calculated using the equation 3.22. The pressure drop (ΔP) through the venturimeter which is required for the calculation of Q_{th} is measured using a manometer.

Figure 3.26 shows the variation of pressure drop through the venturimeter with the air flow rate.

The calculated C_d values for various Re numbers shown in figure 3.27. However, we did not obtain a curve for the C_d, since we used a pressure transmitter for the measurement of the pressure drop through the venturimeter and we calibrated the output of transmitter according to the real water flow rate. The C_d is included in this calibration. The results is shown in figure 3.28.

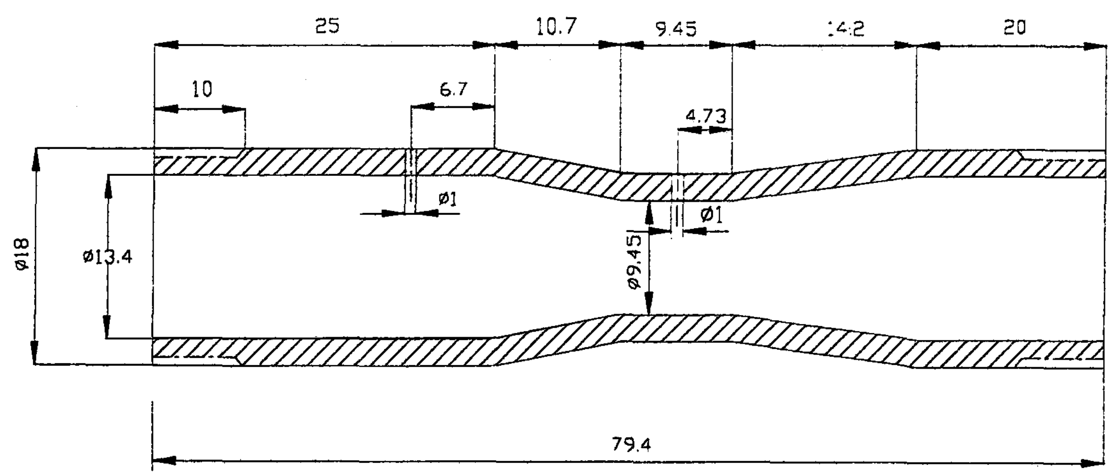

Figure 3.25. Air venturimeter and dimensions

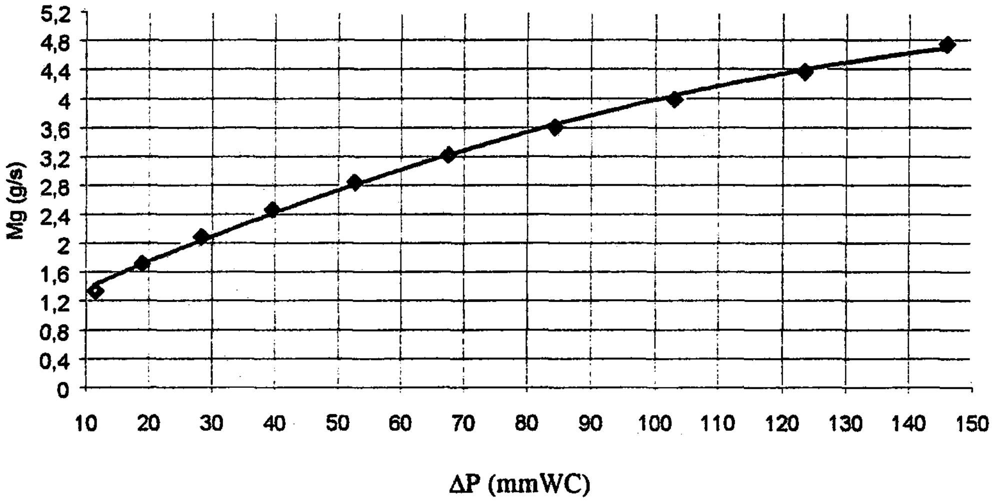

Figure 3.26. Pressure loss and mass flow rate of air in the venturimeter.

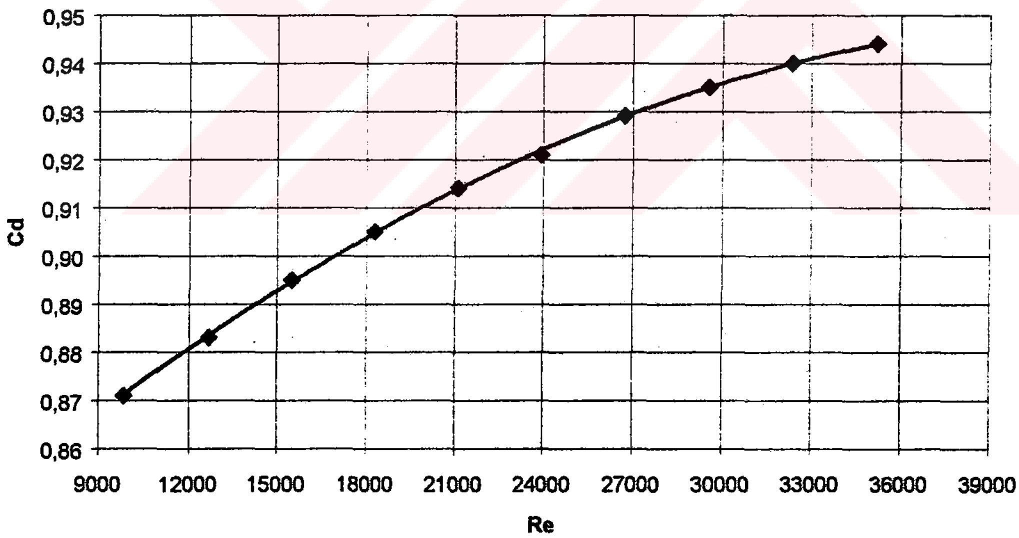

Figure 3.27. Variation with Re of discharge coefficient

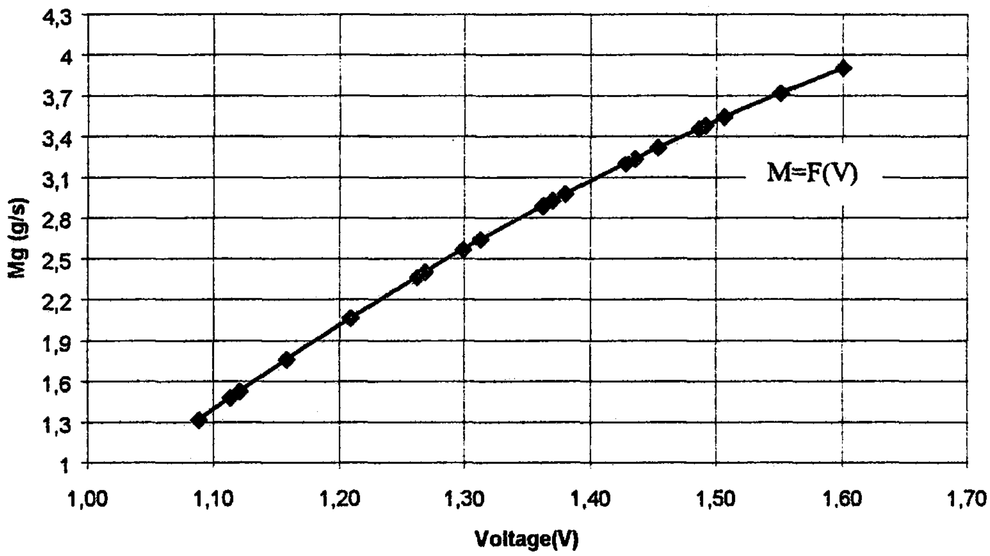

Figure 3.28. Voltage output of the pressure transmitter for various values of flow rate of air

3.4.5.5. Data Acquisition System

Most of the readings on the system are performed using a data logger (P.A. Hilton Ltd.). The data logger's interface is a multi-channel analogue and digital unit with both input and output capability. Commands and data are transferred via 5 wire RS232 serial link using ASCII character string sent and received by a controlling computer.

33 L	+5 V
39 L	-5 V
52	+ 12 V
53	+ 12 V
80	+ 12 V
81	+ 15 V
83	- 15 V

Figure 3.29. The terminals on data logger board

The data logger unit has five on board DC voltage supplies available via the front connector bank. The terminals are labeled (figure 3.29) as follows:

Terminal 81 (+15 V) is used for supplying voltage to the pressure transmitter used for the flow rate measurements.

4. RESULTS AND DISCUSSIONS

In this study, two groups of experiments were performed. The first group was carried out with empty test pipe and the second with various inserts in the test pipe. The results of the first group experiments were compared with the empirical models which are explained in the third section. The second group of experiments were carried out for investigating the effects of various inserts on the structure and the pressure loss of two phase slug flow. The results of the second group of experiments were compared with that of empty pipe conditions.

4.1. FIRST GROUP of EXPERIMENTS

In the first group, the experiments were carried out with empty pipe (no insert in the test section). During the experiments, for the each increased step of water flow rate, air flow rate is varied from the minimum to maximum value.

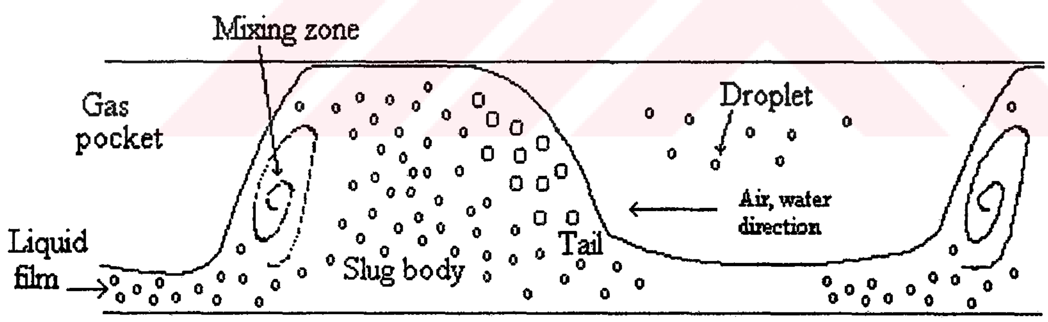

Figure 4.1. Basic image of a slug

A basic image of a slug is shown in figure 4.1. The shape of slug and its parts change with the flow rates of air and water. When the water flow was constant and air flow rate was increased, the parameters of slug changed as fallow;

- The liquid film thinned
- Gas pocket increased
- Slug body length decreased

- Frequency of slug increased
- Bubbles in slug liquid body increased
- Droplets in gas pocket increased and a thin film on the inner surface are seen

During the experiments, pressure loss and flow rates of air and water were measured. This process was performed for five different water flow rates (1.4 kg/s, 1.58 kg/s, 1.80 kg/s, 2.10 kg/s, 2.35 kg/s). The pressure loss between 13th and 15th taps was measured. The distance between these taps is 83 cm. The pressure loss is measured 2 minutes long, one reading each second. The air and water flow rates were measured in 1 minute long, again reading each second. The average values of flow rate and pressure values were collected. Variation of pressure loss for unit pipe length with gas mass flow rate is shown in figure 4.2 for 5 different water mass flow rate.

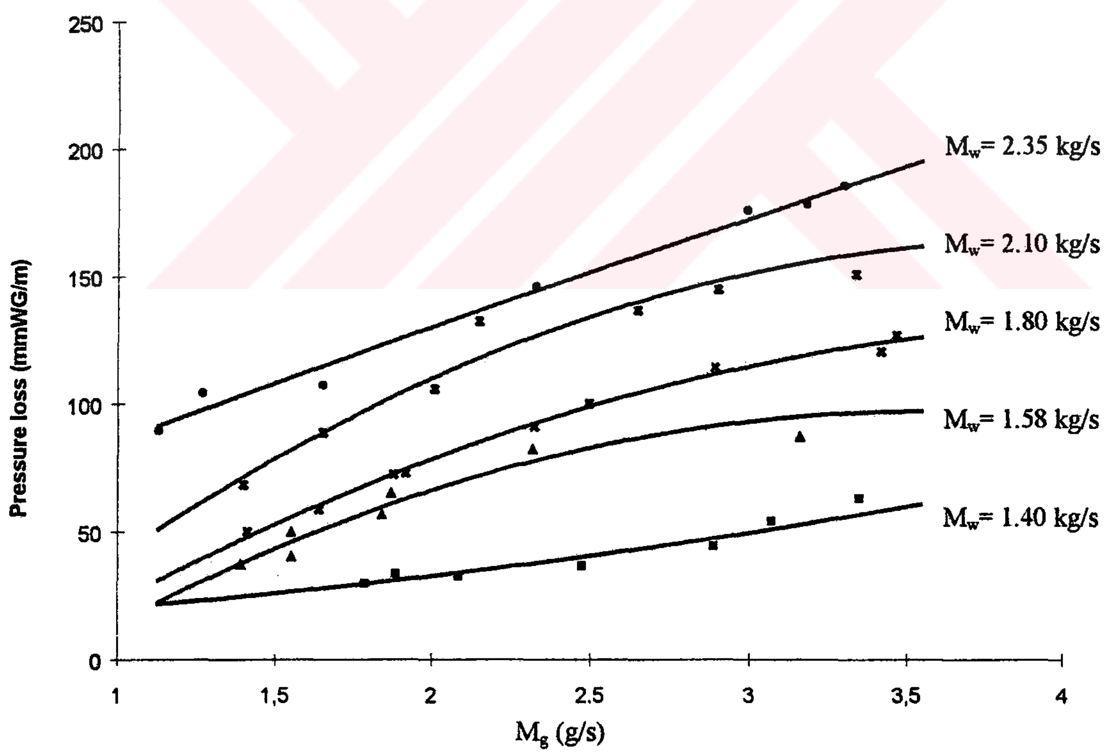

Figure 4.2. Variation of pressure loss with gas flow rate for different water flow rates (no insert)

As it is seen in figure 4.2, pressure loss increases with both increasing air flow rate and increasing water flow rate. The fluctuation in pressure loss for a given water flow rate is thought to be due to the small variations in water flow rate. Although care was given to keep the water flow rate constant, it was impossible to obtain a constant water flow rate due to experimental arrangement used.

The experimentally obtained pressure loss values are compared with the values obtained from different models given in chapter 3.2 in figures 4.3 to 4.7.

In figure 4.3 the experimental values for a water flow rate of 1.40 kg/s are compared with the corresponding values calculated from Lockhart-Martinelli, Chisholm and Boroczy –Chisholm.

As can be seen from this figure, there are big differences between the results. All the empirical models produce higher values then the experimental ones. The results of LMM and BCM coincide with each other, however they are smaller then that of CM which is the highest one. However, all of the models capture the trend that when the gas flow rate is increased, the pressure loss increases.

The pattern is similar in the case of higher water flow rate values although there are differences in term of actual values. For higher water flow rates, CM continue to produce higher values and the very good agreement between the results of LMM and BCM are still evident. However the results of LMM and BCM approach to the experimental ones when the water flow rate is increased especially for higher values of gas flow rate.

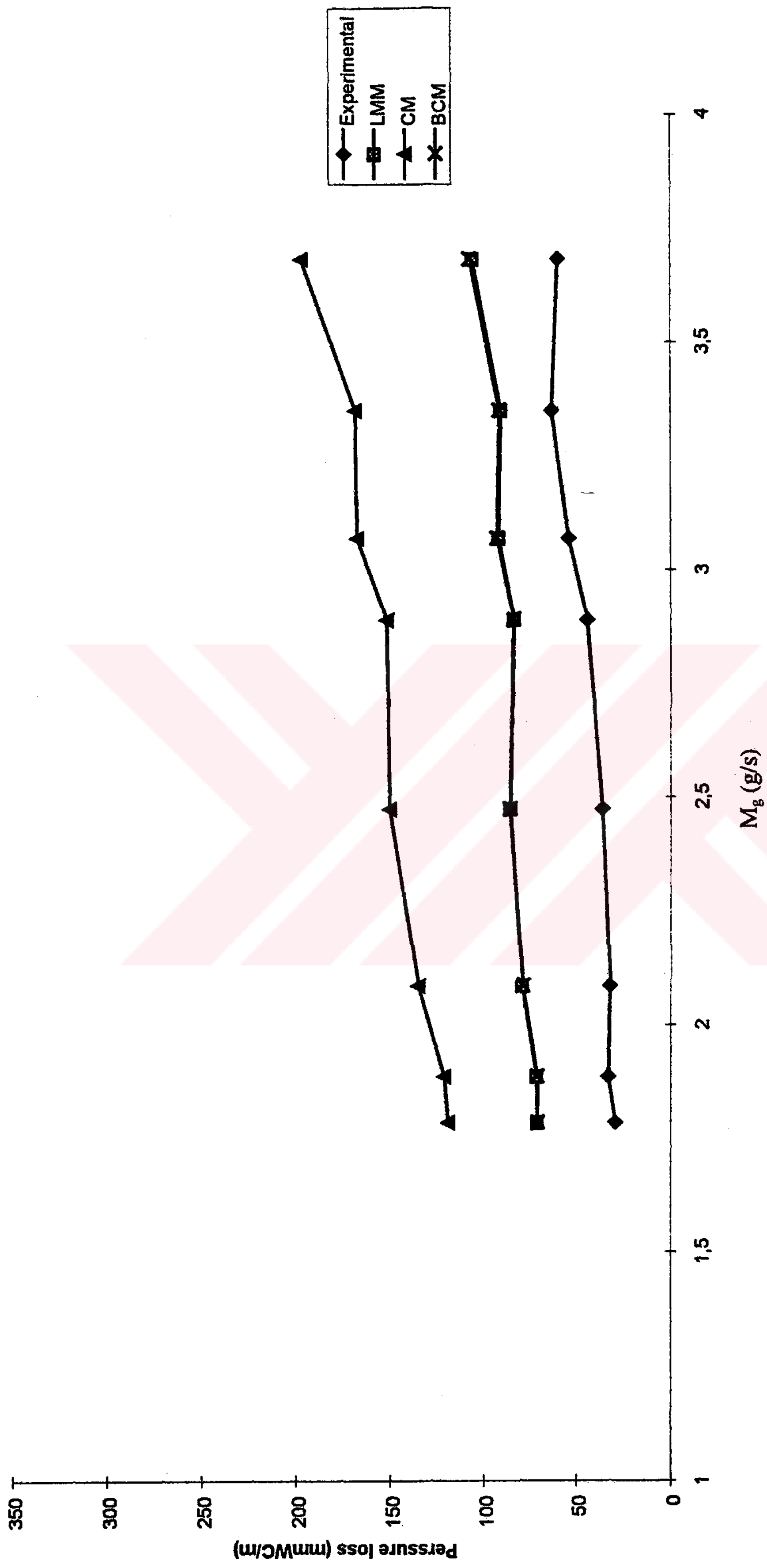

Figure 4.3. Comparison among the experimental pressure loss and Lockhart - Martinelli Method, Chisholm Method and Boroczy - Chisholm Method for M_w=1.40 kg/s (no insert).

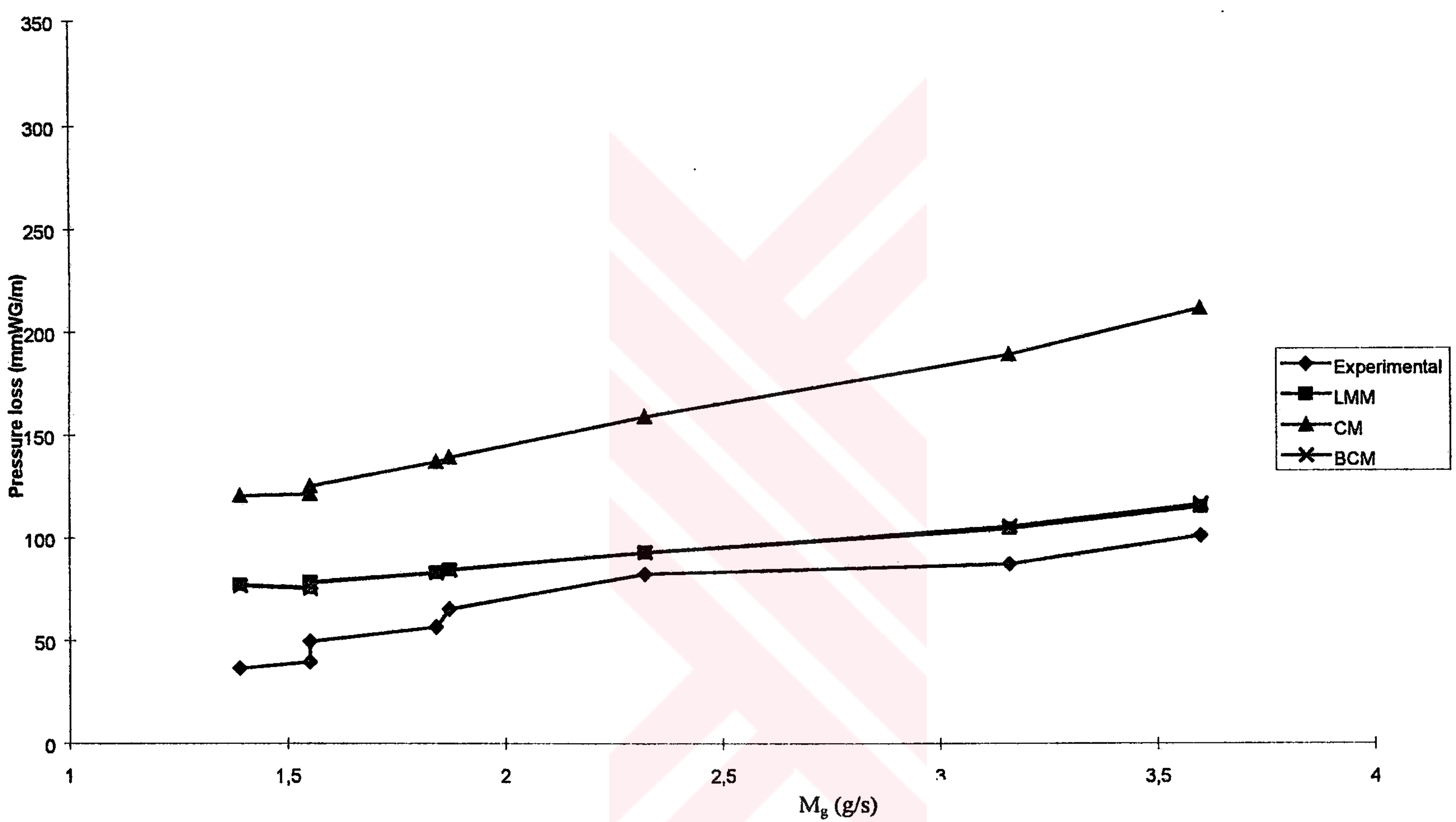

Figure 4.4. Comparison among the experimental pressure loss and Lockhart - Martinelli Method, Chisholm Method and Boroczy –Chisholm Method for M_w =1.55 kg/s (no insert).

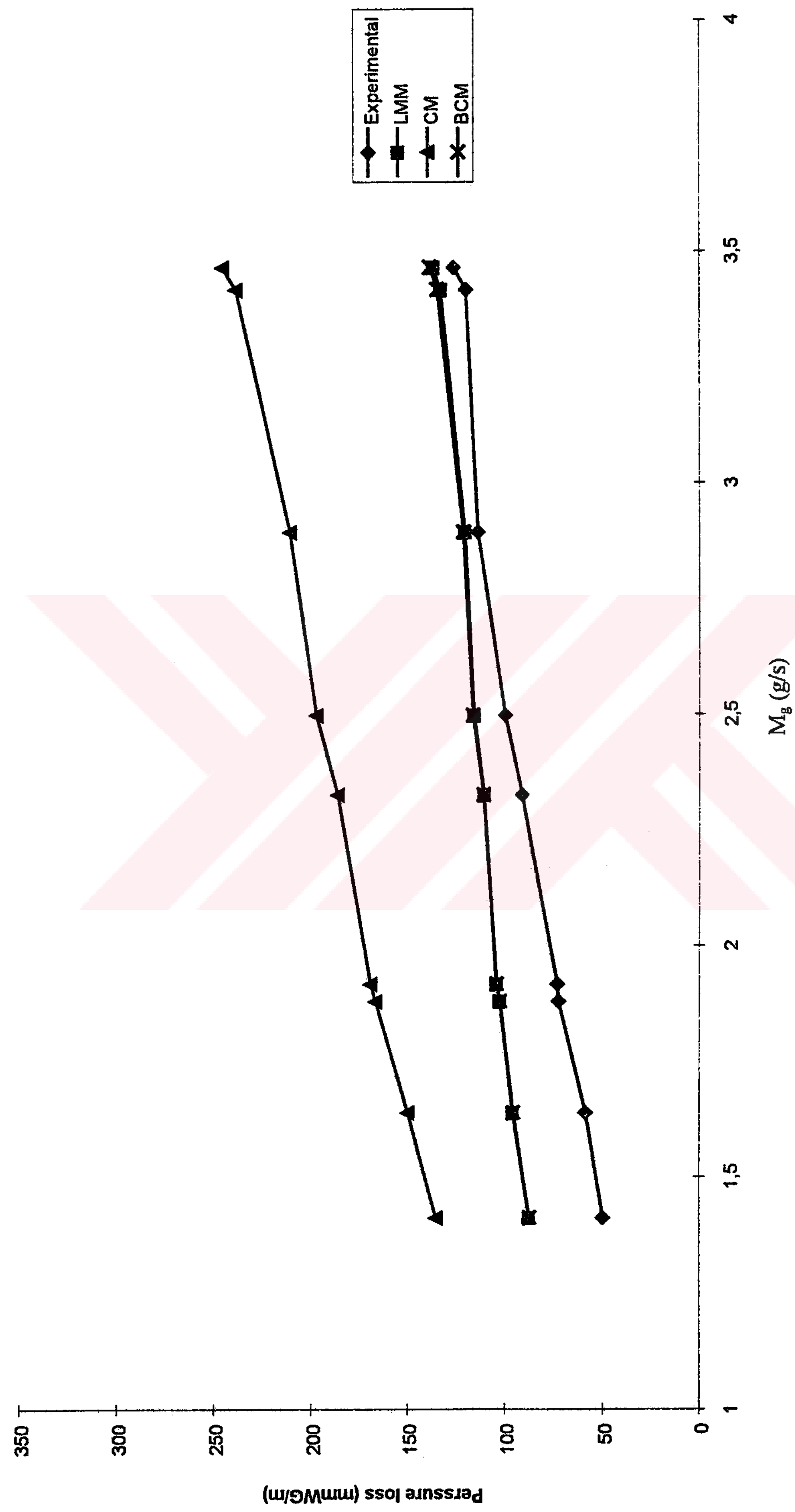

Figure 4.5. Comparison among the experimental pressure loss and Lockhart - Martinelli Method, Chisholm Method and Boroczy - Chisholm Method for M_w =1.80 kg/s (no insert).

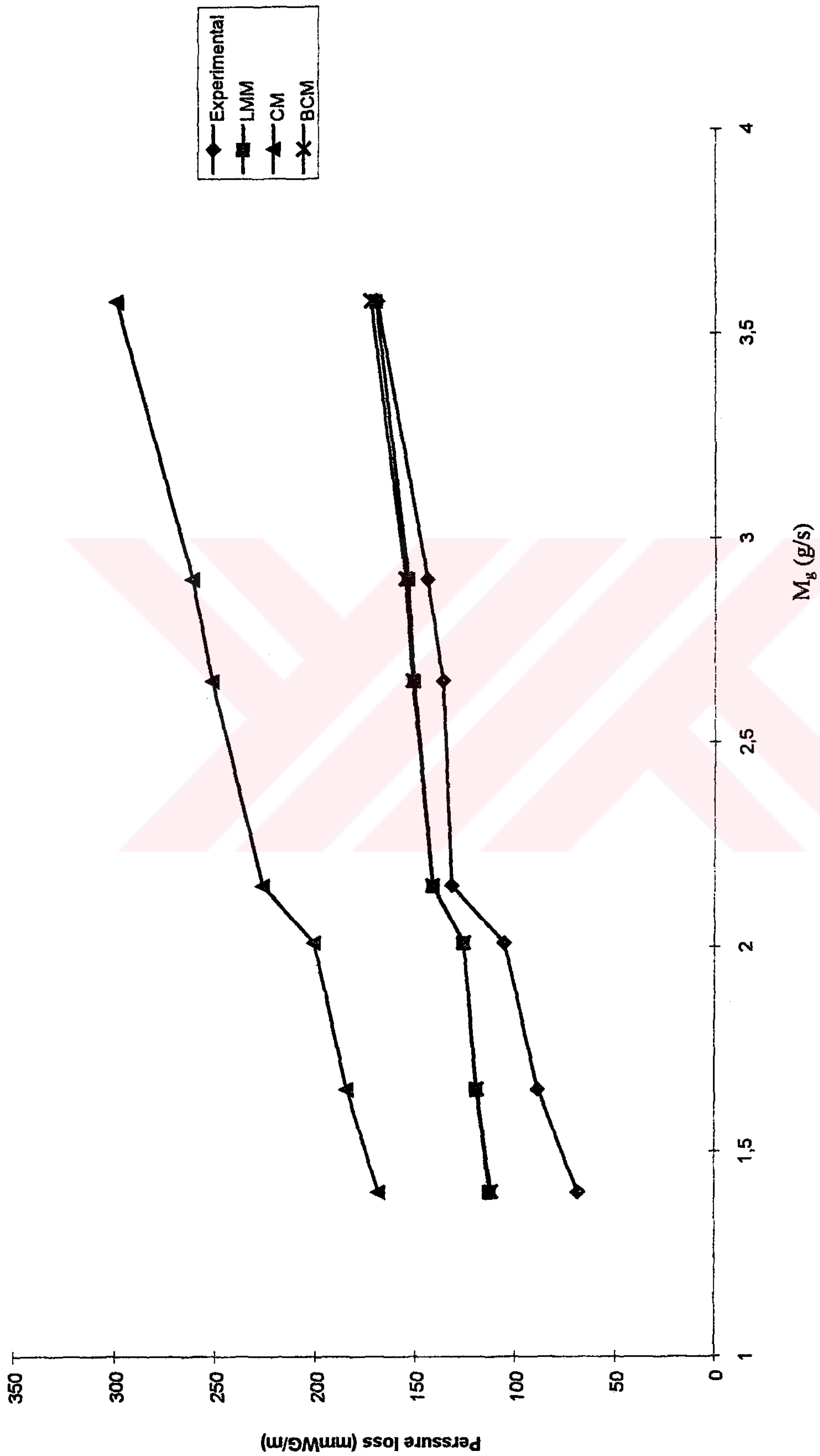

Figure 4.6. Comparison among the experimental pressure loss and Lockhart - Martinelli Method, Chisholm Method and Boroczy - Chisholm Method for M_w= 2.10 kg/s (no insert).

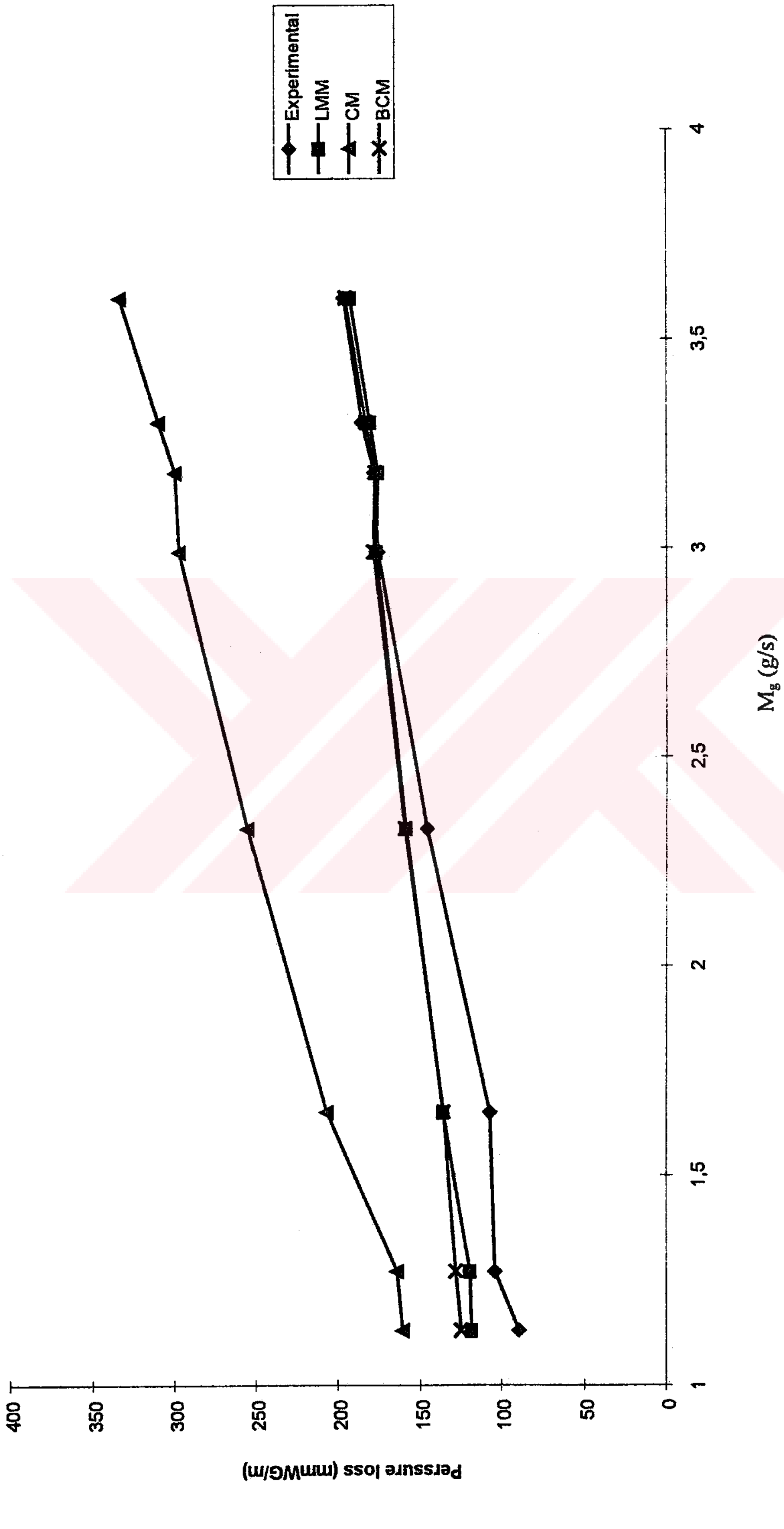

Figure 4.7. Comparison among the experimental pressure loss and Lockhart - Martinelli Method, Chisholm Method and Boroczy - Chisholm Method for M_w= 2.35 kg/s (no insert).

4.2. SECOND GROUP of EXPERIMENTS

In the second group of experiments, various types of inserts were inserted in the test tube. The inserts were replaced into the test tube in two different positions. Firstly they were replaced to the center and then at a position above the centerline. For each condition, experiments were performed for three different water flow rates. In each experiment, the air flow rate, water flow rates and the pressure loss in the test pipe were measured. The pressure loss is measured 2 minutes long and one reading is registered for each second. The air and water flow rates were measured in 1 minute long and again one reading is registered for each second. This time, the pressure loss were measured between the taps 13th and 14th which are 41.5 cm apart form each other.

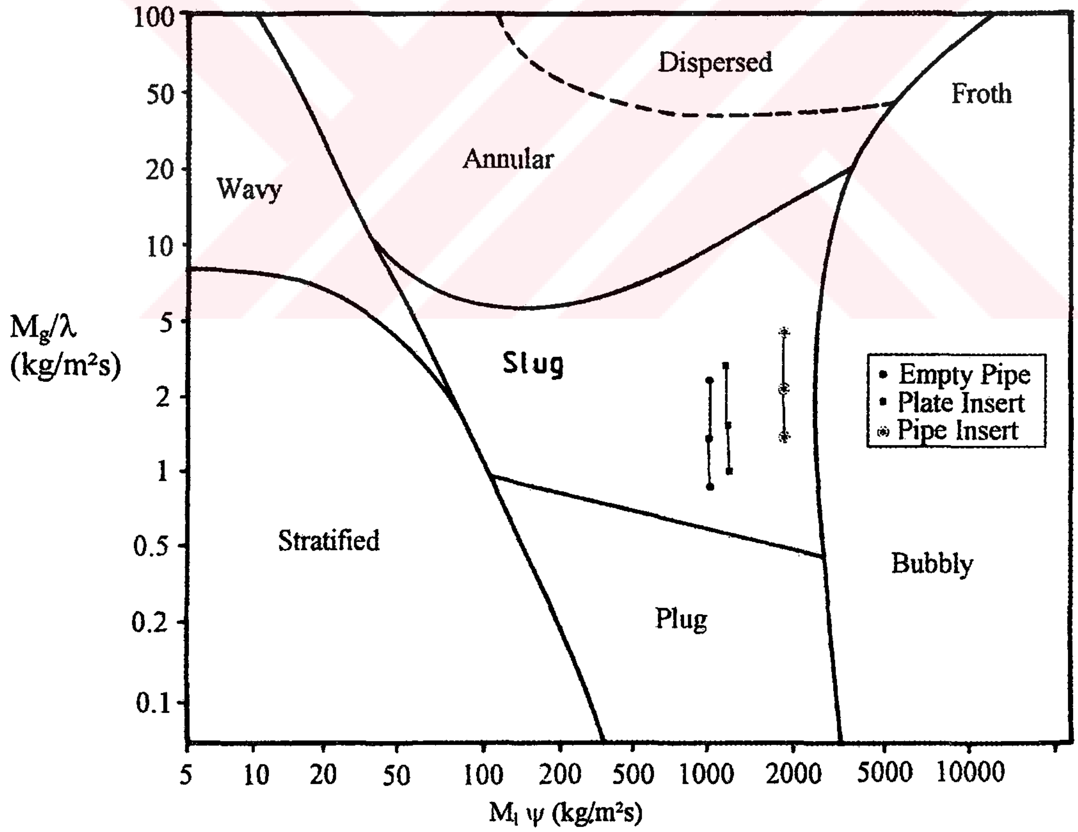

Figure 4.8. Experimental results for three different insert condition (M_w=1.55 kg/s)

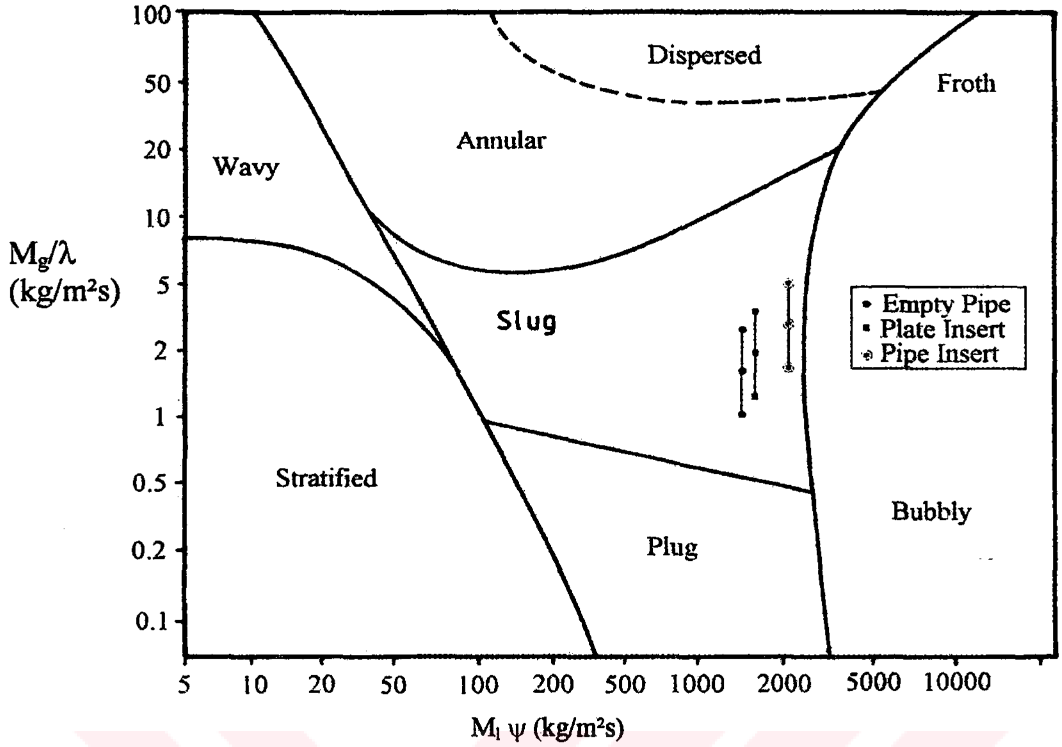

Figure 4.9. Experimental results for three different insert condition (M_w=2.10 kg/s)

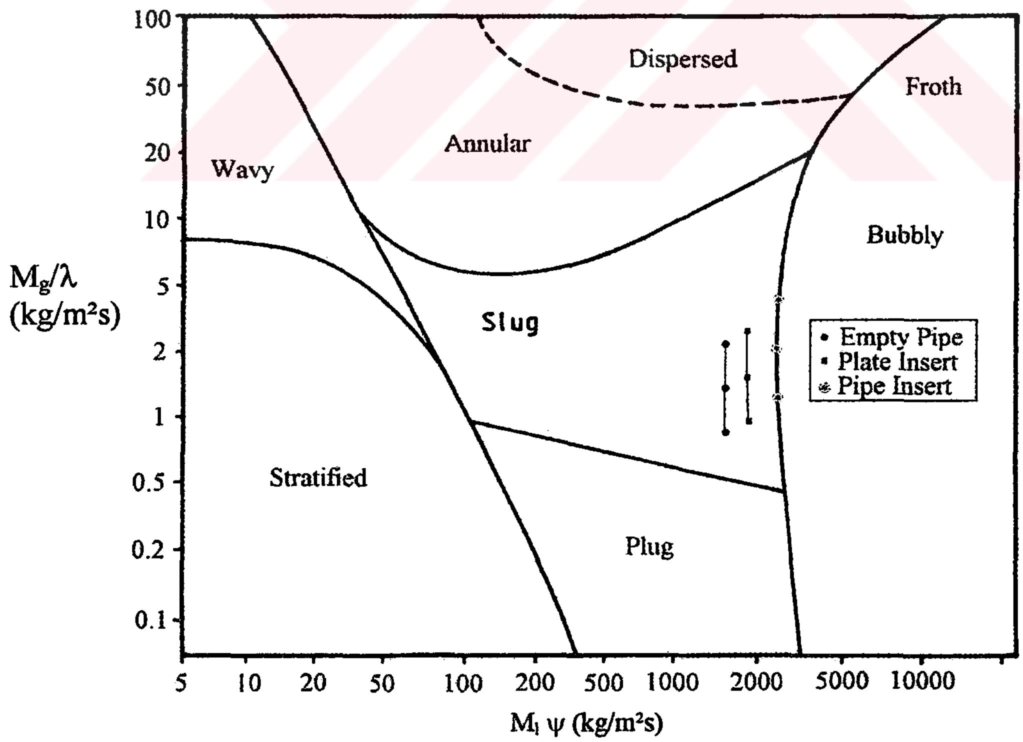

Figure 4.10. Experimental results for three different insert condition (M_w=2.35kg/s)

The experimentally obtained results are compared with the values obtained for three different insert conditions(Empty pipe, Plate insert, Pipe insert) in figure 4.8. to 4.10. As it can be seen in these figures, the flow type changes if an insert is replaced. When the plate insert is replaced, flow type changes from slug flow through annular and bubbly flow. This effect is seen for the pipe insert for much more than the plate insert.

The first insert tested was a two meter long plexiglass plate. It was replaced to the center of the test tube with the help of pin supports. The views of the plate insert at the center of the tube is shown in figure 4.11. The plate was fitted by five pins. Experiment were performed under these conditions. As water flow rate is increasing, average pressure loss is also increasing. In this experiment, variation of air flow rate for three different water flow rate values were measured and values are demonstrated in figures.

Variation of the pressure loss with air flow rate for different water flow rates are shown in figure 4.12. As it can be seen, for M_w=1.55 pressure loss is increasing slowly until M_g=3.2 g/s. After this value, it is increasing rapidly. For water mass flow rate of 2.10 kg/s, until the air flow rate become 2.1 g/s, the pressure loss is increasing slowly. After this value, it is increasing rapidly but it is approaching to a certain pressure loss value. For water mass flow rate of 2.35, the pressure loss are increasing rapidly but approaching to a constant value.

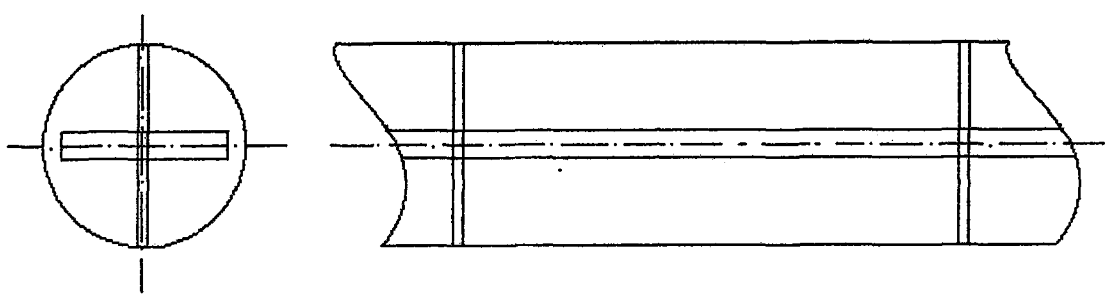

Figure 4.11. The views of the plate insert at the center of the test pipe

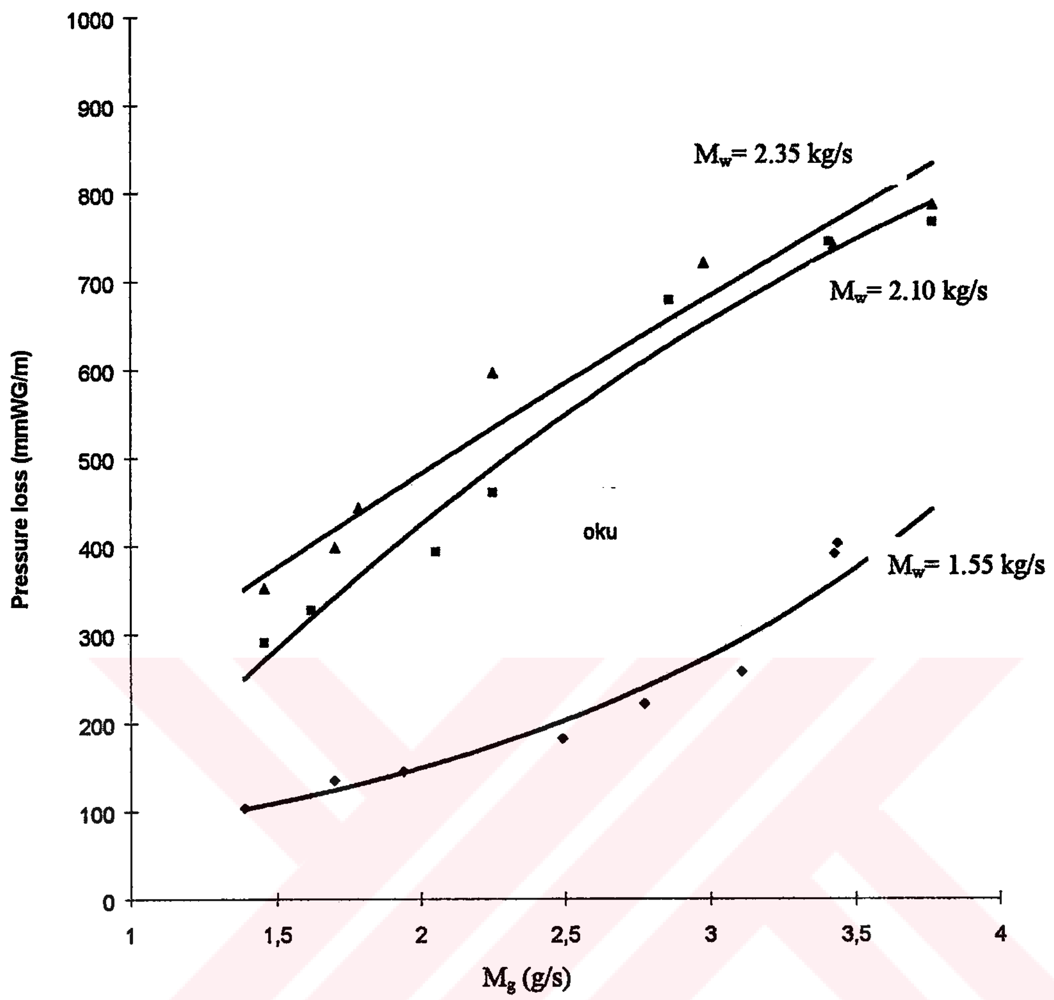

Figure 4.12. Variation of pressure loss with air flow rate for three different water flow rates (plate insert at the center of the tube)

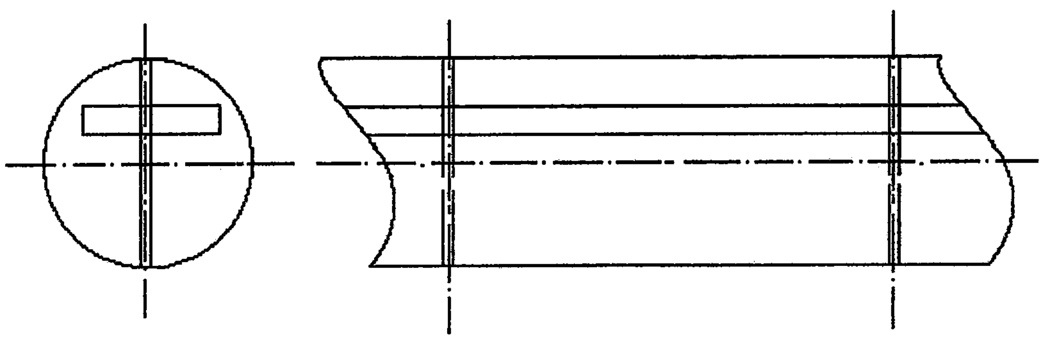

Figure 4.13. Eccentric plate inserted pipe

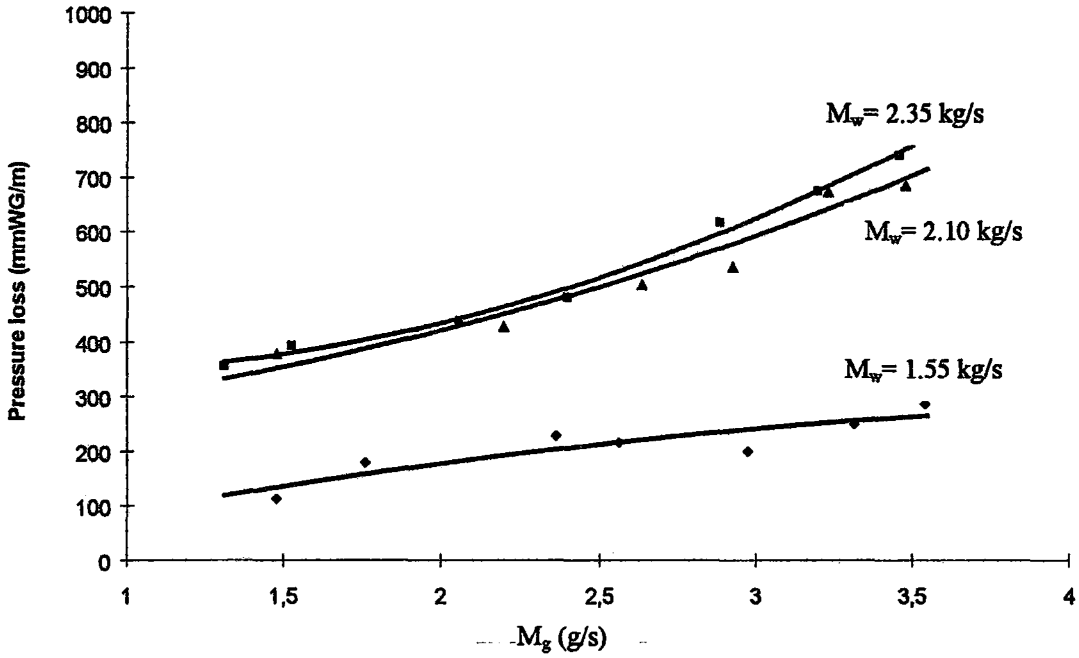

Figure 4.14. Variation of pressure loss with air flow rate for three different water flow rates (plate insert above the centerline of the tube)

In the second experiment, two meters long plexiglass plate insert was replaced at a position above the centerline of the test tube. The views of this condition is shown in figure 4.13. In this experiment, changing of air flow rate for three different water flow rate values were measured and results are shown in figure 4.14. As it can be seen, pressure loss for M_w =1.55 are increasing as linear. For the mass flow rate of water is 2.10 kg/s, until the air flow rate becomes 2.4 g/s, pressure loss is increasing slowly. After this value, they are increasing rapidly. For the water mass flow rate of 2.35, the pressure loss is also increasing rapidly.

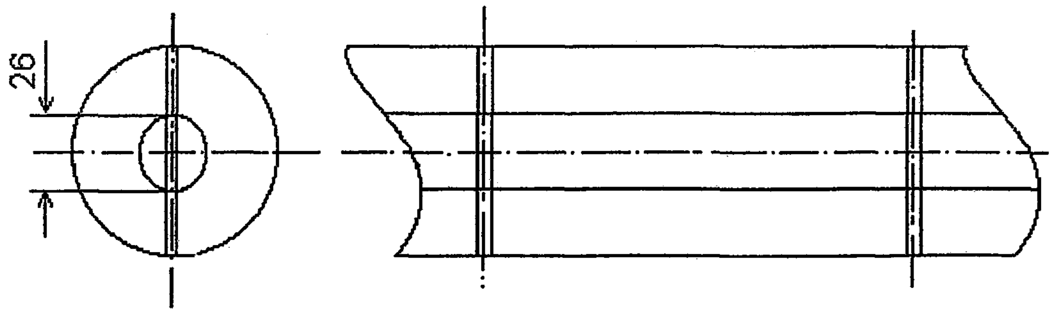

Figure 4.15. The views of the pipe insert at the center of the test pipe

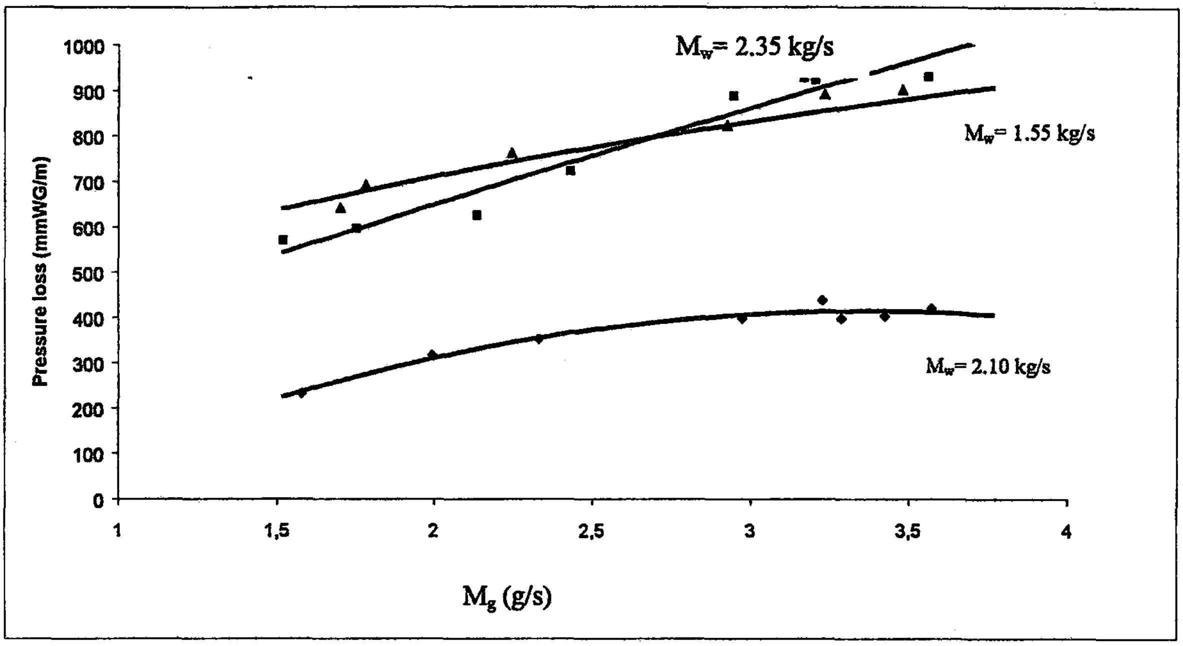

Figure 4.16. Variation of pressure loss with air flow rate for three different water flow rates (pipe insert at the center of the tube)

The third insert tested was a four meters long of plastic pipe. It was replaced to the center the test tube with the help of pin supports. The views of the pipe insert at the center of the test pipe are shown in figure 4.15. Experiments were performed under these conditions and shown in figure 4.16. Pressure loss is increasing slowly for M_w =1.55 and approaching to a constant pressure loss value. For the water mass flow rate of 2.10 kg/s, until the air flow rate becomes 2.1 g/s, pressure loss is increasing slowly. After this value, it is increasing rapidly until the air flow rate becomes 2.8 g/s. After all, the values are approaching to a constant value.

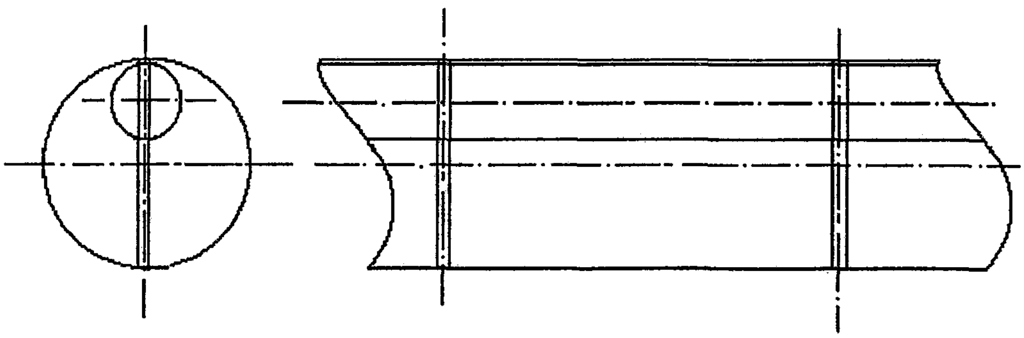

Figure 4.17. The views of the eccentric pipe insert of the test pipe

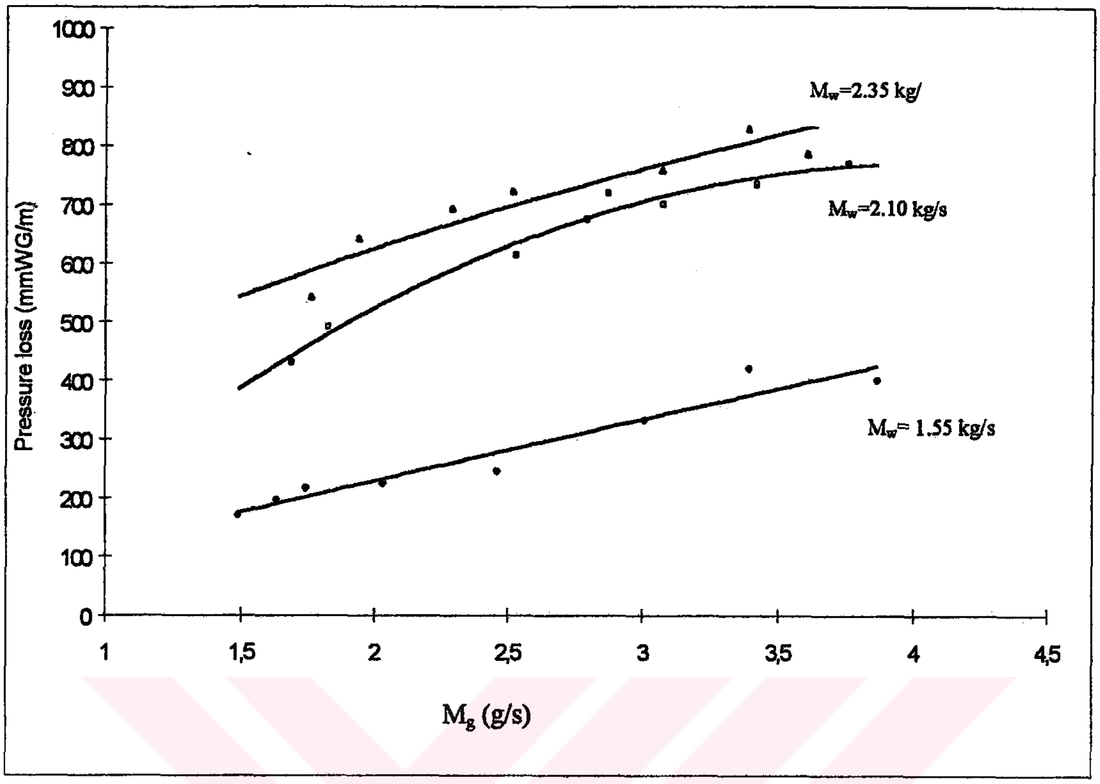

Figure 4.18. Variation of pressure loss with air flow rate for three different water flow rates (pipe insert above the centerline of the tube)

The fourth insert tested was a four meters long of plastic pipe. It was replaced at a position above the centerline with the help of pin supports. Eccentric inserted pipe is shown in figure 4.17. In this experiment, measured values are demonstrated in figure 4.18. As seen, pressure loss for M_w =1.55 are increasing slowly until the air flow rate value becomes 3 g/s. After this value, they are increasing rapidly and then approaching to a constant pressure loss value. For the water mass flow rate of 2.10 kg/s, the pressure loss is increasing rapidly and it is approaching to a constant pressure loss value. For the water mass flow rate of 2.35 kg/s, the pressure loss is increasing more rapidly and it is approaching to a constant pressure loss value.

After all these experiments, it is needed to show the variation of pressure loss with air flow rates for 5 insert conditions in a figure. This is done for three different water flow rates. The pressure loss and air flow rate variations for the water flow rate of 1.55 kg/s are shown in figure 4.19. As seen, average pressure loss is lowest for the test tube without an insert. Until the air flow rate takes the value of 2.5 g/s, pressure loss of the plate insert at the center of the tube are higher than without inserted tube but lower than the other insert conditions. After this value, pressure loss is increasing very rapidly and getting the highest value. For eccentric plate inserted tube, pressure loss values are increasing slowly and linear. The slope of this curve and the average pressure loss are higher than those of non-inserted tube. For the pipe inserted at a position above of the centerline, firstly it has been observed that the pressure loss is increasing slowly and linearly and then it is increasing rapidly. Finally it is approaching to a constant value. The average value of pressure loss of this condition is higher than the others, but not than that of central inserted pipe. The pressure loss of the tube with the central inserted pipe is higher than the others and approaching to a value of pressure loss that are lower than for the plate insert at the center of the test tube and close to the pipe with insert at a position above centerline of the test tube.

The variations of the pressure loss and the air flow rate for the water flow rate of 2.10 kg/s are shown in figure 4.20. As it can be seen that pressure loss is lowest for non-inserted test tube. Pressure loss of the plate insert at the center of tube are higher than that of a tube without an insert and increasing linearly which has a greatest slope. Average values of pressure loss that contribute this curve are less than the other insert conditions. For the tube eccentrically inserted plate, the pressure loss values are increasing rapidly and the slope of it is increasing while air flow rate is increasing. For the tube which is inserted eccentrically, the pressure loss is increasing but approaching to a constant value. The average value of the pressure loss for this condition is higher than the others but not for the pipe which has a pipe insert. The pressure loss of the pipe with a central insert are higher than the others and approaching to a value of pressure loss which are higher than that of the tube eccentrically inserted pipe.

The pressure loss and air flow rate changes for the water flow rate of 2.35 kg/s are shown in figure 4.21. As it can be seen from this figure, pressure loss is lowest for non-inserted test tube. Pressure loss of the tube with a plate insert at the center of the tube are higher than without inserted tube and is approaching to a constant value. The average value of pressure loss is greater than eccentric plate inserted and non-inserted tube. For eccentric plate inserted tube, pressure loss values are increasing linearly up to a constant value. After this value, the slope of this curve is increasing with the increasing of air flow rates. For eccentric pipe inserted tube, pressure loss is increasing but approaching to a constant value. The average value of pressure loss of this condition is higher than the others.

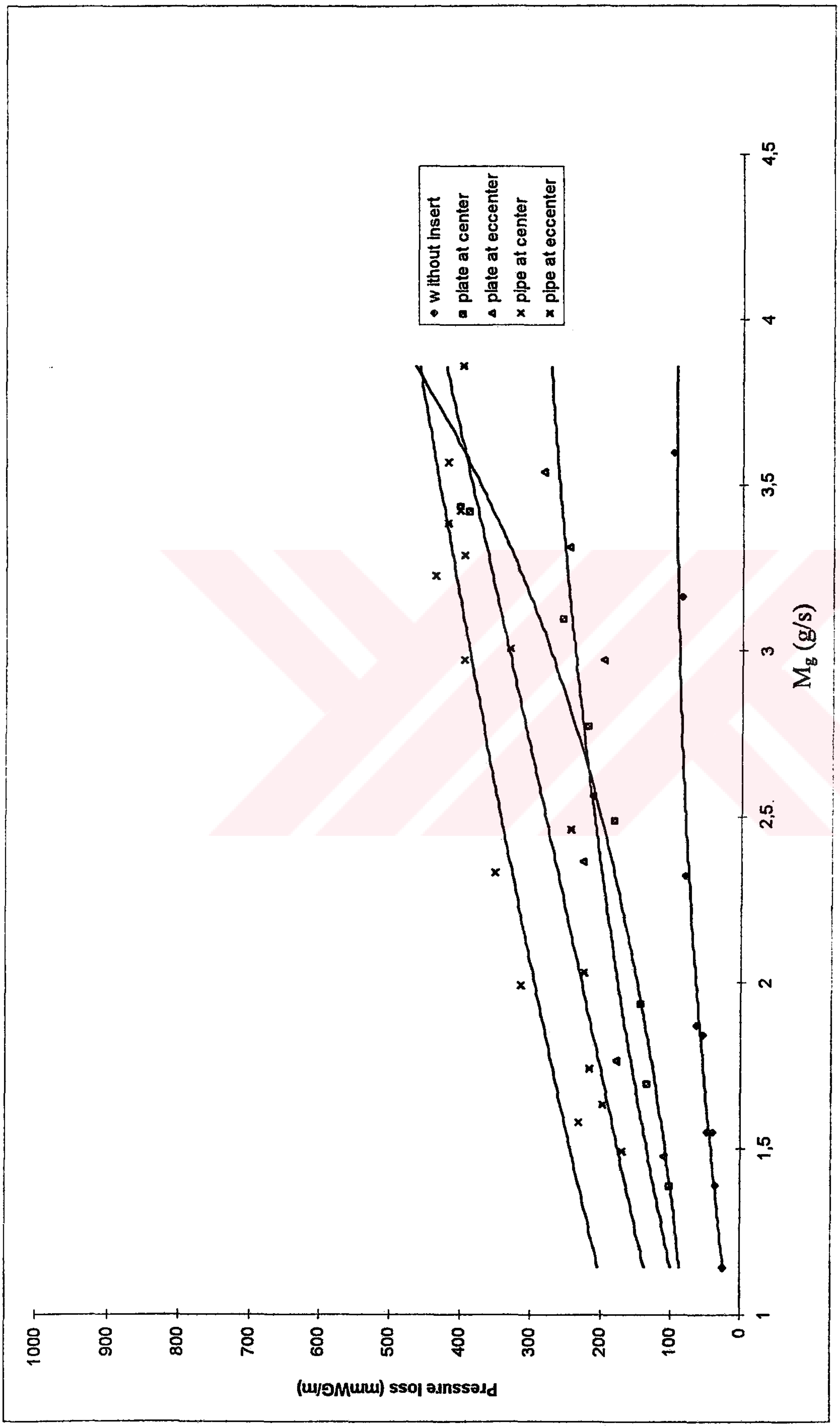

Figure 4.19. Variation of pressure loss with air flow rate for empty pipe and four different insert conditions (M_w =1.55 kg/s)

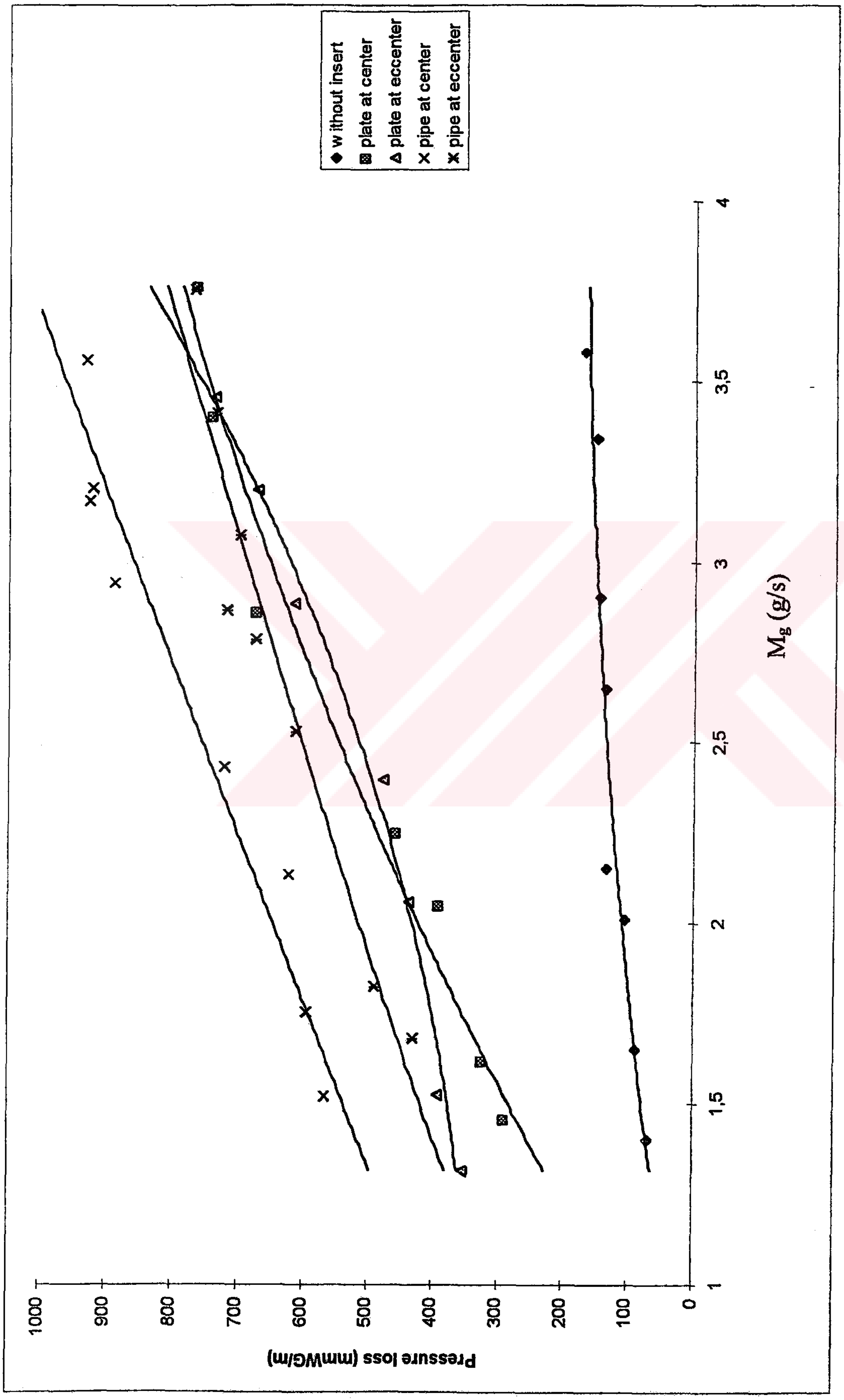

Figure 4.20. Variation of pressure loss with air flow rate for empty pipe and four different insert conditions (M_w=2.10 kg/s)

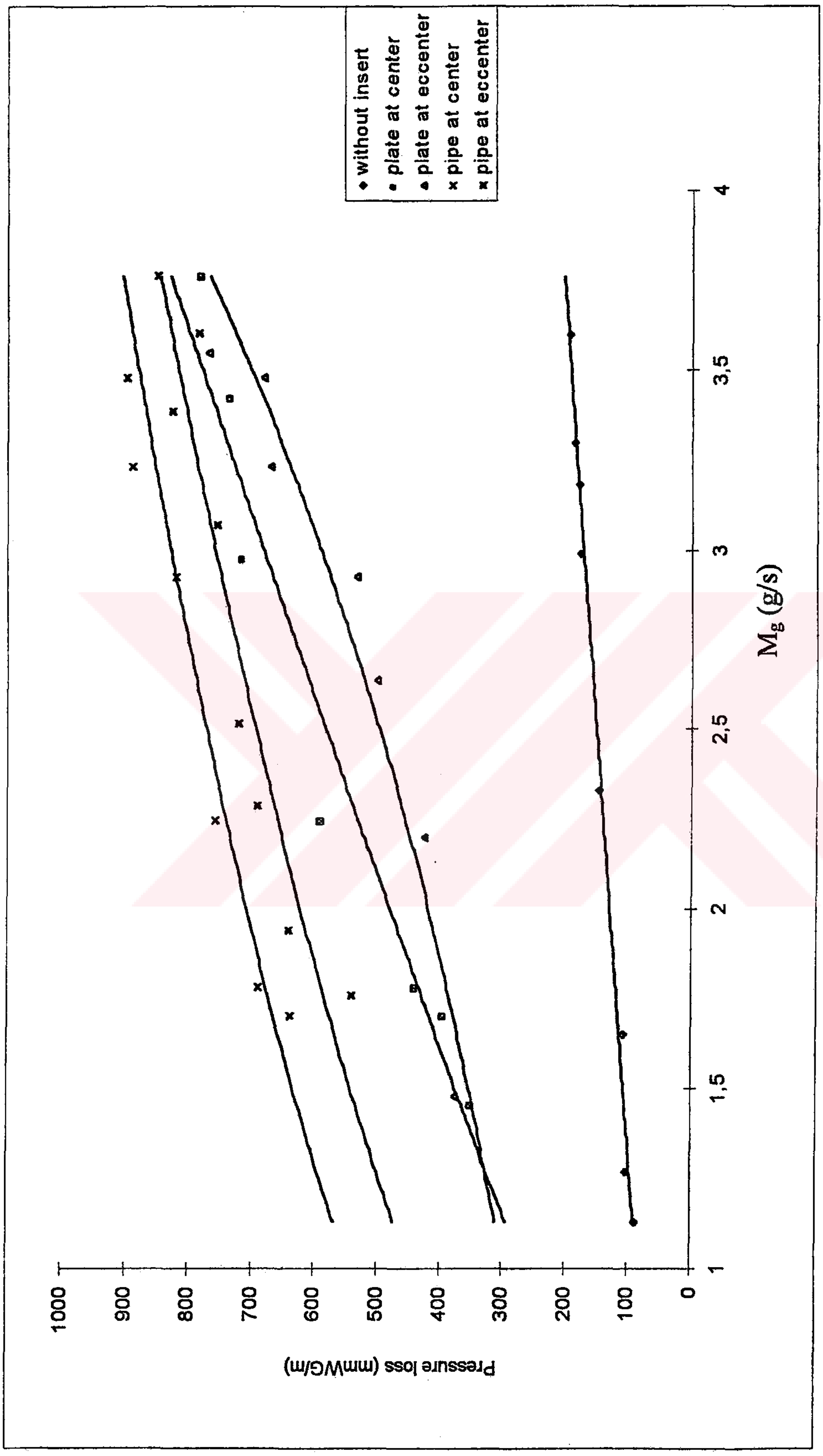

Figure 4.21. Variation of pressure loss with air flow rate for empty pipe and four different insert conditions (M_w=2.35 kg/s)

5. CONCLUSION

The requirement of economic designs, optimization of operating conditions, and assessment of safety factors leads to the need for quantitative information for two-phase flow takes place in a wide range of industrial plant. Slug flow is a very common occurrence in gas-liquid two-phase pipe flow. Due to momentum of the slugs, mechanical forces and vibrations can occur in the pipe system. Approaching eigen frequency of the pipe system, the slug frequency can couse resonance. Such conditions develop to increase pipe damage from internal corrosion and mechanical impacts. For example, pumps are subjected to very strong fluctuations that can have destructive effects in a pipeline. Two-phase flow is not a subject that can be treated successfully by purely theoretical methods. Therefore, many researchers have tackled to get reliable experimental data to determine the flow patterns, pressure drop, velocity distribution and void fraction in tubes. Two-phase gas liquid flows can occur in pipes that should be vertical, horizontal or inclined configurations.

In this study, two groups of experiments were performed. First groups were made without inserted test pipe and second with inserted test pipe. As a results, the outputs of first experiment is used to compare with the empirical methods. There are big differences between the results. All the empirical models produce higher values then the experimental ones. The results of LMM and BCM coincide with each other, however they are smaller then that of CM which is the highest one. However, all of the models capture the trend that when the gas flow rate is increased, the pressure loss increases. The pattern is similar in the case of higher water flow rate values although there are differences in term of actual values. For higher water flow rates, CM continue to produce higher values and the very good agreement between the results of LMM and BCM are still evident. However the results of LMM and BCM approach to the experimental ones when the water flow rate is increased especially for higher values of gas flow rate.

In the second groups of experiments, effects of insert on slug flow were examined. As a result, at plate insert conditions, pressure losses are increasing while air flow rate is increasing. At high water flow rates, slug flow is effected by this type of insert. It is seen that the shape of slug flows transient to bubbly flow but this effects were not seen at low water flow rates by eyes. As a conclusion of pipe inserted condition, pressure losses are approaching a constant values while air flow rate is increasing. The shape of slugs are converting to bubbly flow.

REFERENCES

YILMAZ, T., 1998, Process technologies in gas-liquid flows, Ç.Ü., June 1998, Adana.

KAKAÇ,S. & MAYINGER, F., 1976, Two Phase Flows and Heat Transfer. USA.

BACHALO, W.D., 1994, Experimental methods in multiphase flows. *Int. J. Multiphase Flow. Vol. 20, Suppl., pp. 261-295.*

IIDA, Y., 1980, Prediction method of flow patterns in gas-liquid two-phase flow. *Bulletin of the JSME, Vol. 23. No. 176, pp. 247-254.*

McQUILLAN, K.W. & WHALLEY, P.B., 1985, Flow patterns in vertical two-phase flow. *Int. J. Multiphase Flow, Vol. 11, No. 2, pp. 161-175.*

KOCAMUSTAFAOGULLARI, G., HUANG, W.D. & RAZI, J., 1994, Measurement and modelling of average void fraction, bubble size and interfacial area, *Nuclear Engineering and Design, 148, pp. 437-453.*

SHENG, Y.Y. & IRONS, G.A., 1991., A combined laser doppler anemometry and electrical probe diagnostic for bubbly two-phase flow, *Int.J.Multiphase Flow. Vol. 17. No. 5, pp. 585-598.*

DIN, H.N., SHOOK, C.A. & CORWELL, J., 1987, A conductivity probe for measuring local concentrations in slurry systems, *Int. J. Multiphase Flow. Vol. 13. No. 3, pp. 365-378.*

BARNEA, D. & TAITEL Y., 1993, A model for slug length distribution in gas-liquid slug flow, *Int. J. Multiphase Flow. Vol. 19, No. 5, pp. 829-838.*
NAKORYAKOV, V.E., KASHINSKY, O.N. & KOZMENKO, B.K., 1986,.

Experimental study of gas-liquid slug flow in a small-diameter vertical pipe, *Int. J. Multiphase Flow. Vol. 12, No. 3, pp. 337-355.*

COSTIGAN, G. & WHALLEY, P.B., 1997, Slug flow regime identification from dynamic void fraction measurements in vertical air-water flows, *Int. J. Multiphase Flow, Vol. 23, No. 2, pp. 263-282.*

BARNEA, D. & SHEMER, L., 1989, Void fraction measurements in vertical slug flow: Applications to slug characteristics and transition. *Int.J.Multiphase Flow, Vol.15, No. 4, pp. 495-504.*

BRAUNER, N. & BARNEA, D., 1986, Slug/churn transition in upward gas-liquid flow, *Chemical Engineering Science, Vol. 41. No. 1, pp. 159-163.*

KAWAKAMI, Y., SHIMIZU, H., FUKANO, T. & SEKOGUCHI, K., 1980, Film thickness in gas-liquid two-phase flow, *Bulletin of JSME, Vol.23. No.178, pp.545-552.*

FORE, L.B. & DUKLER, A.E., 1995, The distribution of drop size and velocity in gas-liquid annular flow, *Int. J. Multiphase Flow, Vol. 21, No. 2, pp. 137-149.*

LIU, T.J. & BANKOFF S.G., 1993, Structure of air-water bubbly flow in a vertical pipe-I. Liquid mean velocity and turbulence measurements, *Int. J. Multiphase Flow, Vol. 36, No. 4, pp. 1049-1060.*

LIU, T.J. & BANKOFF S.G., 1993, Structure of air-water bubbly flow in a vertical pipe-II. Void fraction, bubble velocity and bubble size distribution, *Int. J. Multiphase Flow, Vol. 36, No. 4, pp. 1061-1072.*

JABARDO, J.M.S. & BOURE, J.A., 1989., Experiments on void fraction waves, *Int. J. Multiphase Flow, Vol. 15, No. 4, pp. 483-493.*

WHALLEY, P.B., 1980, Air-water two-phase flow in a helically coiled tube, *Int. J. Multiphase Flow, Vol. 6, pp. 345-356.*

SAXENA, A.K., SCHUMPE, A., NIGAM, K.D.P. & DECKWER, W.D., 1990, Flow regimes, hold-up and pressure drop for two phase flow in helical coils. *The Canadian J. of Chem. Engineering. Vol. 68, pp. 553-559.*

WATANABE, O., NAKAJIMA, K. & FUJITA, H., 1993, Characteristics of liquid-film thickness of air-water annular two-phase in helically coiled tubes, *Heat Transfer-Japanese Research. 22(5), pp. 447-461.*

SADATOMI, M., SATO, Y. & SARUWATARI, S., 1982, Two-phase flow in vertical noncircular channels, *Int. J. Multiphase Flow, Vol. 8, No. 6, pp. 641-655.*

SEKOGUCHI, K., FUKANO, T., KAWAKAMI, Y., SHIMIZU, H. & FURUKAWA, T.,1981, Gas-liquid two-phase flow in double-tubes-annular-passage with flow obstruction, *Bulletin of JSME, Vol. 24. No. 189, pp. 562-570.*

KELESSIDIS, V.C. & DUKLER, A.E., 1989, Modeling flow pattern transitions for upward gas-liquid flow in vertical concentric and eccentric annuli, *Int. J. Multiphase Flow, Vol. 15, No. 2, pp. 173-191.*

CHOI, K.Y. & NO, H.C. 1995, Experimental studies of flooding in nearly horizontal pipes, *Int. J. Multiphase Flow, Vol. 21. No. 3, pp. 419-436.*

BARNEA, D. & TAITEL, Y., 1993, A model for slug length distribution in gas-liquid slug flow, *Int. J. Multiphase Flow, Vol. 19. No. 5, pp. 829-838.*

TRONIEWSKI, L. & ULBRICH, R., 1984, Two-phase gas-liquid flow in rectangular channels, *Chem. Eng. Science, Vol. 39. No. 4, pp. 751-765.*

AWWAD, A., XIN, R.C., DONG, Z.F., EBADIAN, M.A.& SOLIMAN, H.M., 1995, Measurement and correlation of the pressure drop in air-water two-phase flow in horizontal helicoidal pipes, *Int.J. Multiphase Flow, Vol.21. No.4, pp.607-619.*

STANISLAV, J.F., KOKAL, S. & NICHOLSON, M.K., 1986, Gas liquid flow in downward and upward inclined pipes, *The Canadian J. of Chemical Engineering, Vol. 64, pp. 881-890.*

ANDREUSSI, P. & BENDIKSEN, K., 1989, An investigation of void fraction in liquid slugs for horizontal and inclined gas-liquid pipe flow, *Int. J. Multiphase Flow, Vol. 15. No. 6, pp. 937-946.*

CURRICULUM VITEA

Bahri BÜYÜKAKÇALI was born in Kadirli, 1975. He finished his primary, secondary and high school education in Adana. He gained his Bachelor of Science in Çukurova University Mechanical Engineering Department in 1997. On completion of his degree, he started his Master of Science studies in Çukurova University, Institute of Natural and Applied Sciences, Mechanical Engineering Division. He still works as a Research Assistant in this Division.

CURRICULUM VITEA

Bahri BÜYÜKAKÇALI was born in Kadirli, 1975. He finished his primary, secondary and high school education in Adana. He gained his Bachelor of Science in Çukurova University Mechanical Engineering Department in 1997. On completion of his degree, he started his Master of Science studies in Çukurova University, Institute of Natural and Applied Sciences, Mechanical Engineering Division. He still works as a Research Assistant in this Division.

Table 4. Experimental data of figure 4.3

M_g (g/s)	M_w (kg/s)	ΔP (Experimental)	ΔP (LMM)	ΔP (CM)	ΔP (BCM)
1,79	1,42	29,62	71,2	119	70,8
1,89	1,40	33,33	71,6	121	71,3
2,09	1,46	32,48	79,2	135,1	79
2,47	1,46	36,48	85,7	150,3	85,9
2,89	1,34	44,27	83,5	151,8	84
3,07	1,41	53,99	91,8	167,3	92,5
3,35	1,40	62,94	90,6	168,2	91,4
3,68	1,46	59,57	105,8	197	107,1

Table 5. Experimental data of figure 4.4

M_g (g/s)	M_w (kg/s)	ΔP (Experimental)	ΔP (LMM)	ΔP (CM)	ΔP (BCM)
1,39	1,52	37,03	77	120,5	76,4
1,55	1,55	40,08	75,5	121,3	75
1,55	1,59	49,72	78,2	125,1	77,7
1,84	1,55	56,59	83	137,1	82,8
1,87	1,54	65,07	84,3	139,5	84,1
2,32	1,59	82,22	92,8	159,1	92,9
3,16	1,55	87,01	104,7	189,3	105,6
3,60	1,52	101,00	115	211,3	116,4

Table 6. Experimental data of figure 4.5

M_g (g/s)	M_w (kg/s)	ΔP (Experimental)	ΔP (LMM)	ΔP (CM)	ΔP (BCM)
1,41	1,77	49,93	87,6	135,5	87,1
1,64	1,85	58,70	96,2	150,1	95,8
1,88	1,84	72,41	103	167	102,8
1,92	1,85	72,96	104,6	169,6	104,5
2,33	1,82	91,18	111	186,6	111,3
2,50	1,84	100,07	116,2	197,3	116,7
2,89	1,80	114,08	120,8	210,9	121,7
3,42	1,81	120,26	133,2	238,4	134,8
3,47	1,85	126,45	136,9	245,2	138,6

Table 7. Experimental data of figure 4.6

M_g (g/s)	M_w (kg/s)	ΔP (Experimental)	ΔP (LMM)	ΔP (CM)	ΔP (BCM)
1,4	2,11	68,49	112,9	168,6	111,9
1,65	2,12	88,73	119,6	184,4	119,3
2,01	2,09	105,64	126	201	126
2,15	2,23	132,18	141,4	226,7	141,7
2,65	2,2	136,54	151,1	252	152,1
2,9	2,17	144,58	154,3	261,9	155,6
3,58	2,17	169,61	170,2	299,3	172,6

Table 8. Experimental data of figure 4.7

M_g (g/s)	M_w (kg/s)	ΔP (Experimental)	ΔP (LMM)	ΔP (CM)	ΔP (BCM)
1,13	2,37	89,53	118,4	160,8	124,8
1,27	2,36	104,13	119,5	164,2	128,2
1,65	2,32	107,23	136,1	206,6	135,8
2,33	2,37	146,02	158,7	255,5	159,4
2,99	2,38	175,68	176,7	297,3	178,5
3,18	2,32	178	175,6	299,7	177,6
3,3	2,34	185,26	180,6	309,8	182,8
3,6	2,38	196	192,3	333,7	195,1

Table 9. Experimental data of figure 4.8

M_w (kg/s)	M_g (g/s)	$X_{(empty)}$ (kg/m^2s)	$Y_{(empty)}$ (kg/m^2s)	$X_{(plate\ insert)}$ (kg/m^2s)	$Y_{(plate\ insert)}$ (kg/m^2s)	$X_{(pipe\ insert)}$ (kg/m^2s)	$Y_{(pipe\ insert)}$ (kg/m^2s)
1,55	1,14	1230,69	0,91	1339,41	0,99	2019,54	1,49
1,62	1,39	1286,99	1,11	1400,69	1,20	2111,94	1,82
1,55	1,55	1234,62	1,23	1343,69	1,34	2025,99	2,02
1,59	1,55	1263,55	1,23	1375,18	1,34	2073,47	2,02
1,58	1,84	1258,92	1,47	1370,13	1,60	2065,86	2,41
1,59	1,87	1265,24	1,49	1377,02	1,62	2076,24	2,44
1,59	2,32	1265,00	1,85	1376,75	2,01	2075,84	3,03
1,55	3,16	1231,74	2,52	1340,56	2,74	2021,27	4,13
1,58	3,60	1259,19	2,86	1370,43	3,12	2066,30	4,70

2,29	3,42			739,25
2,34	1,78			442,24
2,34	2,25			594,87
2,35	3,76			784,62
2,35	2,98			718,62
2,36	1,46			351,49
2,38	1,70			396,87

Table 13. Experimental data of figure 4.14

M_w (kg/s)	M_g (g/s)	ΔP (M_w =1,55)	ΔP (M_w =2,10)	ΔP (M_w =2,35)
1,53	2,56	215,36		
1,55	2,97	198,86		
1,55	3,54	285,49		
1,57	1,76	178,24		
1,57	1,48	112,24		
1,58	2,36	227,74		
1,58	3,31	248,37		
2,14	2,06		438,12	
2,15	2,40		479,37	
2,15	3,46		739,25	
2,16	3,20		673,25	
2,18	1,31		355,62	
2,18	2,88		615,50	
2,21	1,53		392,74	
2,32	1,48			376,7462
2,33	2,20			425,5924
2,36	3,48			683,4538
2,36	3,23			671,6117
2,37	2,64			501,34
2,37	2,92			533,6031
2,45	3,55			770,6453

Table 14. Experimental data of figure 4.16

M_w (kg/s)	M_g (g/s)	ΔP (M_w =1,55)	ΔP (M_w =2,10)	ΔP (M_w =2,35)
1,56	2,33	351,82		
1,56	1,99	315,53		
1,59	1,58	231,01		
1,75	3,23	438,12		
1,80	3,29	396,87		
1,83	2,97	396,87		
1,86	3,57	420,36		

1,88	3,42	402,97		
2,03	3,17		927,34	
2,04	3,20		920,97	
2,06	3,56		929,89	
2,07	2,94		887,24	
2,18	2,43		721,60	
2,23	2,13		623,75	
2,37	1,75		595,79	
2,39	1,52		567,83	
1,88	1,70			640
2,04	1,78			690
2,06	2,25			760
2,07	2,92			820
2,18	3,23			890
2,23	3,48			900
2,37	3,76			850

Table 15. Experimental data of figure 4.18

M_w (kg/s)	M_g (g/s)	ΔP (M_w =1,55)	ΔP (M_w =2,10)	ΔP (M_w =2,35)
1,56	2,03	225,26		
1,57	1,63	196,81		
1,57	1,74	216,72		
1,58	3,01	332,69		
1,58	2,46	245,14		
1,59	1,49	169,48		
1,62	3,39	420,50		
1,72	3,86	400,00		
1,98	3,76		769,19	
2,03	3,41		735,17	
2,08	3,07		701,15	
2,08	2,79		675,73	
2,10	2,87		719,15	
2,12	2,53		613,53	
2,14	1,82		491,49	
2,17	1,68		430,80	
2,22	3,61			786,29
2,25	3,38			828,67
2,27	3,07			757,38
2,29	2,29			692,78
2,34	2,52			721,67
2,41	1,76			542,25
2,46	1,94			641,28

Table 16. Experimental data of figure 4.19

M_g (g/s)	ΔP (empty pipet)	ΔP (cen. plate insert)	ΔP (ecc. plate insert)	ΔP (cen. pipe insert)	ΔP (ecc. pipe insert)
1,14	25,83				
1,39		103,56			
1,39	37,03				
1,48			112,24		
1,49					169,48
1,55	40,08				
1,55	49,72				
1,58				231,01	
1,63					196,81
1,70		134,50			
1,74					216,72
1,76			178,24		
1,84	56,59				
1,87	65,07				
1,94		144,81			
1,99				315,53	
2,03					225,26
2,32	82,22				
2,33				351,82	
2,36			227,74		
2,46					245,14
2,49		181,93			
2,56			215,36		
2,77		221,12			
2,97				396,87	
2,97			198,86		
3,01					332,69
3,10		257,40			
3,16	87,01				
3,23				438,12	
3,29				396,87	
3,31			248,37		
3,39					420,50
3,42				402,97	
3,43		390,25			
3,44		402,62			
3,54			285,49		
3,57				420,36	
3,60	101,00				
3,86					400,00

Table 17. Experimental data of figure 4.20

M_g (g/s)	ΔP (empty pipet)	ΔP (cen. plate insert)	ΔP (ecc. plate insert)	ΔP (cen. pipe insert)	ΔP (ecc. pipe insert)
1,31			355,62		
1,4	68,49				
1,46		290,56			
1,52				567,83	
1,53			392,74		
1,62		326,74			
1,65	88,73				
1,68					430,80
1,75				595,79	
1,82					491,49
2,01	105,64				
2,05		392,74			
2,06			438,12		
2,13				623,75	
2,15	132,18				
2,25		460,25			
2,40			479,37		
2,43				721,60	
2,53					613,53
2,65	136,54				
2,79					675,73
2,86		677,37			
2,87					719,15
2,88			615,50		
2,9	144,58				
2,94				887,24	
3,07					701,15
3,17				927,34	
3,20			673,25		
3,20				920,97	
3,34	150,45				
3,41		743,37			
3,41					735,17
3,46			739,25		
3,56				929,89	
3,58	169,61				
3,76					769,19
3,76		765,62			

Table 18. Experimental data of figure 4.21

M_g (g/s)	ΔP (empty pipet)	ΔP (cen. plate insert)	ΔP (ecc. plate insert)	ΔP (cen. pipe insert)	ΔP (ecc. pipe insert)
1,13	89,53				
1,27	104,13				
1,46		351,49			
1,48			376,7462		
1,65	107,23				
1,70		396,87		640	
1,76					542,25
1,78		442,24		690	
1,94					641,28
2,20			425,5924		
2,25		594,87		760	
2,29					692,78
2,33	146,02				
2,52					721,67
2,64			501,34		
2,92			533,6031	820	
2,98		718,62			
2,99	175,68				
3,07					757,38
3,18	178				
3,23			671,6117	890	
3,3	185,26				
3,38					828,67
3,42		739,25			
3,48			683,4538	900	
3,55			770,6453		
3,6	196				
3,61					786,29
3,76		784,62		850	